ACS Catalysis

Perspective

pubs.acs.org/acscatalysis

Local Environment and Nature of Cu Active Sites in Zeolite-Based Catalysts for the Selective Catalytic Reduction of NO_x

Upakul Deka,[†,‡] Ines Lezcano-Gonzalez,[†,‡] Bert M. Weckhuysen,*[,‡] and Andrew M. Beale*[,‡]

[†]Materials Innovation Institute (M2i), Mekelweg 2, 2628 CD Delft, The Netherlands

[‡]Inorganic Chemistry and Catalysis Group, Utrecht University, Universiteitsweg 99, 3584 CA, Utrecht, The Netherlands

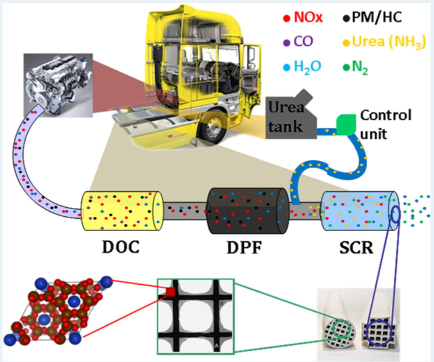

ABSTRACT: Cu-exchanged zeolites have demonstrated widespread use as catalyst materials in the abatement of NO_x, especially from mobile sources. Recent studies focusing on Cu-exchanged zeolites with the CHA structure have demonstrated them to be excellent catalysts in the ammonia-assisted selective catalytic reduction (NH_3-SCR) of NO_x. Thorough characterization of these materials using state-of-the-art techniques has led to a significant improvement in the understanding of active sites present, which contributes toward a fundamental understanding of the catalytic processes and the rational design of new materials; however, the availability of multiple techniques at our disposal has led to various observations and conclusions on the nature of the active sites. This article begins with a brief introduction to exhaust emission control in the mobile sector, followed by an overview of hydrocarbon-SCR and NH_3-SCR; the former technology having found common use in light duty passenger vehicles, whereas the latter are applied for medium (or heavy) duty vehicles, such as trucks and busses. This is followed by an overview of zeolite-based catalysts, especially for NH_3-SCR reaction with a focus toward zeolites known to possess high activity. They include zeolites Y (FAU framework), ZSM-5 (MFI framework), SSZ-13 (CHA framework), and (briefly) zeolite Beta (BEA framework). A few common techniques used for the characterization of zeolites and the information that they bring to help determine the salient structural and mechanistic aspects of the NH_3-SCR process are introduced. The combination and comparison of the information obtained from the approaches have resulted in an accurate elucidation of the local geometry and environment of Cu within zeolites, thus forming the active site. The article further focuses on three main aspects: (a) the crystallographic cation location of Cu within the structures as compared to results from techniques more sensitive to the local environment; (b) the interaction of Cu at these sites with reactant or probe molecules, which illustrates their (potential) mobility and accessibility; and (c) the proposed active sites within the zeolites ZSM-5, Y, and SSZ-13 as evident in literature. The discussion is focused toward the influence of the zeolite structure, from both a long-range perspective and that of the local structure around the active Cu species, on the thus formed active sites and their implications toward the NH_3-SCR reaction.

KEYWORDS: *Cu-zeolites, NH_3-SCR, active sites*

1. INTRODUCTION

Growing concerns over climate change, our ecological footprint, and human health have resulted in local and global measures to control the release of pollutants into our atmosphere. One such measure by the European Commission is the National Emissions Ceilings Directive (NECD), which sets limits on the amount of acidifying and eutrophying pollutants released into the atmosphere from both mobile and stationary sources. The NECD recognizes four main air pollutants, namely: (a) nitrogen oxides (NO_x's), (b) sulfur oxides (SO_x's), (c) nonmethane volatile organic compounds, and (d) ammonia (NH_3).[1−4]

Owing to their efficiency and durability, diesel engines have seen their fair share of use in road transport, especially in the European market. Although slightly more efficient compared to their gasoline counterpart, diesel engines still form air-polluting side products as a consequence of the use of a fossil fuel. In fact, all four air pollutants recognized by the NECD can be formed as a product of combustion in a diesel engine, of which NO_x is of primary concern. Studies within European member countries have confirmed that ~40% of the total NO_x released into the atmosphere comes from road transport alone, of which 75% is from the use of diesel engines.[4,5] The last 20 years have witnessed a decrease of ~95% in NO_x released from heavy duty diesel engines. Figure 1 illustrates the trend of decrease in the amounts of total NO_x and particulate matter in the exhaust stream as per EU legislations. The initial standards merely required fine-tuning the engine to meet the required standards. However, continuous stringent measures (since 2005) have led to the use of catalyst materials as after-treatment solutions to help reduce emissions. With upcoming Euro VI standards (to be implemented in the period 2015−2017), the need to recognize and optimize new catalytic technologies is of significant importance to the automotive industry.

This article presents one such technology: namely, the selective catalytic reduction (SCR) of NO_x in mobile exhaust streams.

Received: December 7, 2012
Revised: January 21, 2013
Published: January 22, 2013

© 2013 American Chemical Society

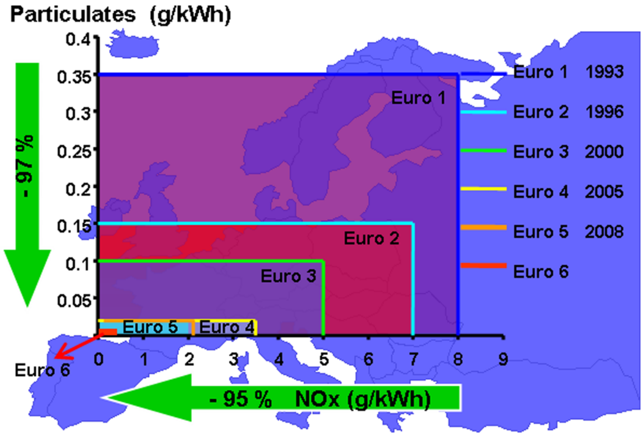

Figure 1. The trend in permitted amounts of NO_x and particulate matter in Europe as set by the European legislation with time. Euro VI, initially planned for 2013, is to be implemented in two stages during the 2015−2017 period.

SCR is an effective and promising technology for the reduction of NO_x gases. In the SCR process, NO_x's are converted into N_2 using a sacrificial reducing agent over a catalyst surface.[5−13] SCR technologies are subcategorized on the basis of the reducing agent used to achieve the same chemical reaction, that is, the breakdown of NO_x into N_2. Two major SCR technologies that have reached or are reaching commercialization are based on hydrocarbon-SCR (HC-SCR) and urea-SCR (also referred to as ammonia-SCR). Perhaps less popular has been SCR technologies using CO or H_2 as a reducing agent,[9] although the latter has been found necessary to enable low-temperature activity in HC-SCR.[14] Section 2 of this article presents a brief introduction into the SCR process using both hydrocarbons (HCs) and ammonia (NH_3) as a reducing agent. Although both are closely related, the article is mainly focused on NH_3-SCR rather than on HC-SCR. Many different catalysts have been studied for this reaction; however, industrial and academic research studies on NH_3-SCR have shown metal-exchanged zeolites to be excellent catalyst materials for this reaction. Particularly, Cu-exchanged zeolites possessing the CHA structure appeared to show excellent activity and selectivity toward the SCR reaction.[15−18] This article therefore discusses the origins of the high activity/selectivity of CHA type systems compared with other commonly applied zeolites: namely, zeolite ZSM-5, zeolite Y, and zeolite Beta.

2. SELECTIVE CATALYTIC REDUCTION

2.1. Hydrocarbon-Selective Catalytic Reduction. As the name suggests, HC-SCR uses hydrocarbons as reducing agent for the SCR reaction. Since a sufficiently large amount of partially burned/unburned HCs are already present in the exhaust stream of diesel engines, this is a very attractive technique for most manufacturers. The use of Cu-zeolites for HC-SCR was realized early in the 1990s.[19,20] One of the earliest systems developed for this purpose by König and co-workers around 1985 at Volkswagen, used a Cu-exchanged mordenite catalyst, which was successful in reducing the concentrations of NO_x in a gas mixture consisting of NO_x, HC (i.e., methane, ethene, propene, or butane), and oxygen. Following these results, the same group tested different metals, including Cu, Cr, Fe, Mn, V, Co, Ni, and Ag, although Cu was found to be the most effective among them. However, this Cu-exchanged mordenite was very sensitive to steam present in the system, which was overcome by changing the support material to zeolite ZSM-5. Nevertheless, this work, along with work performed by Iwamoto et al. around the same time, led to further investigations in the area. As different metals and supports were tested for the same catalytic reactions, Smedler et al. found that Ag/Al_2O_3 was an effective catalyst to reduce NO_x at 400 °C using propane, propene, or alkene as reducing agents.[21] One of the major drawbacks of Ag/Al_2O_3 systems around this time was that they could not operate at lower temperatures. However, the addition of hydrogen appeared to overcome this problem.[22,23] Very recent studies have demonstrated that Ag/Al_2O_3 catalysts prepared via mechanochemical ball-milling are active at temperatures as low at 250 °C, even without the addition of hydrogen.[24] A Pt (or Pd)/Al_2O_3 system was also found to overcome this low-temperature activity problem, however, with the unacceptable drawback of producing large amounts of N_2O, which is a greenhouse gas >300 times worse than CO_2 and additionally responsible for the depletion of ozone.[12]

2.2. Urea or Ammonia-Selective Catalytic Reduction. Ammonia-assisted SCR was already in use during the 1970s,[25] although mainly for stationary applications. When put into mobile applications, the drawback of NH_3 is that it is toxic, corrosive, and a pollutant and, therefore, presents a risk for being transported in pressurized containers. Hence, urea came to be used (as a source for NH_3) in heavy duty trucks and buses.[26] The basic idea behind urea-SCR is to decompose aqueous urea in water to NH_3 via the following reactions:

$$(NH_2)_2CO \rightarrow NH_3 + HNCO \tag{2.1}$$

$$HNCO + H_2O \rightarrow NH_3 + CO_2 \tag{2.2}$$

For the purpose of discussion, urea-SCR will be referred to here as NH_3-SCR, since most research studies (including our own) discussed and presented herein directly use NH_3 gas as the reducing agent. The basic SCR reaction (known as the standard SCR reaction) using ammonia can be described as

$$4NH_3 + 4NO + O_2 \rightarrow 4N_2 + 6H_2O \tag{2.3}$$

Reaction 2.3 proceeds faster in the presence of a 1:1 mixture of NO and NO_2 (designated fast SCR), primarily because NO_2 is a much stronger oxidizing agent than O_2 itself. Furthermore, studies have indicated that NO oxidation over metal zeolites could possibly be the rate-determining step, which is discussed further in the following section. However, a typical diesel engine exhaust contains only a minor fraction of NO_2.

$$4NH_3 + 2NO + 2NO_2 \rightarrow 4N_2 + 6H_2O \tag{2.4}$$

The advantage of having the 1:1 mixture for fast-SCR has led to the implementation of new technologies, such as exhaust gas recycling to increase the amounts of NO_2 in the feed. Diesel oxidation catalysts, which were originally implemented to oxidize CO and unburned hydrocarbons presented in the exhaust feed also helps increase the amounts of NO_2. There are, however, some problems with NH_3-SCR. To mention a few, depending on the conditions, the formation of N_2O or explosive ammonium nitrates has been observed, which affect both emission quality and block catalyst pores leading to deactivation.[27] The formation of the latter can be avoided by maintaining the temperature of the system above 200 °C, although this is not favorable for wide-scale applications.[7] This higher temperature margin is also required to obtain a complete decomposition/hydrolysis of urea to ammonia. Another major hurdle is the reaction between SO_3 (from diesel) and NH_3, which leads to the formation of ammonium sulfates.

These salts accumulate over time and effectively cause irreversible damage to the catalysts. Although the removal of sulfur from diesel is practiced at present, the amount of permitted sulfur varies globally, and therefore, this issue cannot be ignored completely.

From a catalyst perspective, SCR (whether it be HC-SCR or NH_3-SCR) typically uses metal oxides, noble metals, or metal-exchanged zeolites as catalyst materials. Figure 2 illustrates a map of catalyst materials commonly active for SCR compared with the particular temperature ranges of their maximum activity. Although active in the low temperature range (175–250 °C), the drawbacks of noble metals (e.g., Pt), in addition to the formation of N_2O, are their high costs.[12] Metal oxides (especially based on vanadium), although being very effective and popular for stationary SCR applications, are being phased out in mobile applications because of toxicity concerns related to the volatility of vanadia above 650 °C.[7] In addition, there is the problem of the rutile–anatase phase transition of titania, which is known to occur at ~500 °C and could also result in catalyst deactivation. Metal-exchanged zeolites eventually came to receive attention as efficient catalysts in the 1990s.[19,20] Initial concerns related to poisoning or hydrothermal stability did prevent their commercialization for a long time;[13] however, recent developments have clearly demonstrated that metal-exchanged zeolites are highly suitable for NH_3-SCR.[15,28] In addition to their high activity and selectivity toward N_2, zeolites are relatively inexpensive to produce and are nontoxic, which make them excellent candidates for mobile emission control applications.[6,7]

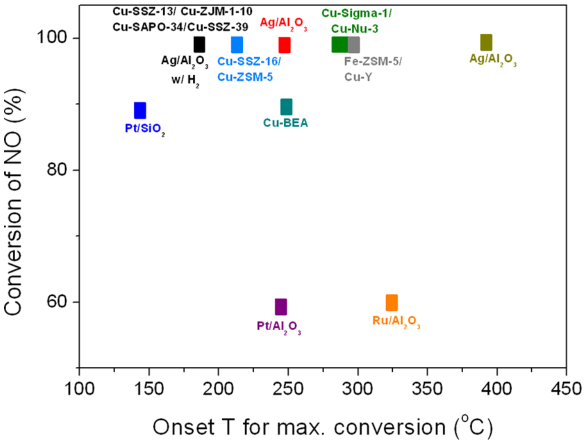

Figure 2. Catalytic materials commonly used and tested for SCR of NO in the presence of different reducing agents. Note: The results obtained are from multiple studies performed in different laboratories and under different conditions.[7,11,12,16,18,29−32] Note: Ag/Al_2O_3 has been illustrated three times in the graph: the first system (black) is representative of the catalytic activity of Ag/Al_2O_3 in the presence of additional H_2, the second (in red) represents the catalytic activity of Ag/Al_2O_3 prepared via a mechanochemical ball-milling approach, and the third (in olive green) represents that of conventionally prepared Ag/Al_2O_3.

2.3. Metal-Exchanged Zeolite Catalysts in NH_3-SCR.

Over the past two decades, multiple combinations of zeolite frameworks with different metals, each with its own pros and cons, has been shown to be active for the SCR reaction. The parent zeolite itself was not found to be as active as its metal (cation-exchanged) counterpart. This was attributed to the fact that the presence of a transition metal ion (TMI) provides a redox catalytic center over the (internal) surface of the zeolite structure.

From a zeolite perspective, zeolites ZSM-5 (MFI framework), Y (FAU framework), mordenite (MOR framework), and Beta (BEA framework) have received the most attention, owing to their already widespread use in related catalysis, easy availability, and framework stability at different temperatures of operation. Over time, it was seen that medium-pore zeolites (e.g., ZSM-5, ferrierite, or mordenite) were more active when compared to larger pore zeolites (e.g., Y, USY, and Beta). More recent studies, particularly between 2008 and 2010, have shown an increasing interest toward zeolites with even smaller pore windows (mainly with the CHA structure) in both the academic and patent literature.[15,16,18,28,33] As a consequence, a lot of interest has been spurred toward the study of these materials in the NH_3-SCR reaction.

Few metals—namely, Cu, Fe, Cr, Ce, and Ag—have now been established as the most effective when compared with others, such as Co, Ni, Mn, Mg, La, and Zn.[7] Cu and Fe have perhaps been the most widely studied TMIs for NH_3-SCR, owing to their availability and high activity. A possible reason can be found in the fact that both Cu and Fe show good redox capacity. Typically, Cu-zeolites were seen to reach the onset of maximum activity at lower temperatures of ~200 °C, whereas Fe-zeolites reached maximum activity at slightly higher temperatures. This effect has been observed and discussed widely in the literature. It has been debated that the Fe-ZSM-5 system is highly dependent on the amounts of NO_2 present in the gas composition, which appears to be the rate-determining step.[34] Furthermore, it has also been demonstrated that the rate of NO oxidation to NO_2 is much lower over Fe-zeolites than the rate of the standard SCR reaction itself.[35] It has also been argued that Fe-based systems suffer from a NH_3 inhibition effect.[36,37] Further comparative studies between commercial Cu- and Fe-exchanged zeolites also showed that Cu-zeolites were less sensitive to the presence of NO_2.[38,39] Therefore, under standard SCR conditions, that is, the absence of NO_2 in the feed, a Cu-zeolite system is expected to show a maximum activity at lower temperatures when compared with a Fe-ZSM-5 system. However, Cu-zeolites are known to oxidize ammonia at temperatures over 350 °C.[7,38,39] A recent investigation on combining the effects of both Cu and Fe used monoliths made up of either metal-exchanged zeolite in different sequential configurations.[40] A system with a 50/50 mixture of a Cu monolith and a Fe monolith appeared to have the same effect as just described. Kucherov et al. performed another study in which they modified a series of Fe-Beta with various amounts of Cu loadings with a similar observation.[41] ESR studies showed that upon addition, Cu^{2+} replaced some of the Fe^{3+} present in their system. The activity profiles suggested that the presence of both metals gave rise to activity over a wider temperature range.

The following sections of the article will discuss the role of various copper species found in zeolites explored for NH_3-SCR. Zeolites Y, ZSM-5, and SSZ-13 (CHA framework) will be the main focus, considering their widespread investigation and efficiency of these materials in the reaction. Although Cu-Beta has also been found to be an active system, the inherent disorder in the BEA framework results so far in a lack of structural information available. As a result, to date, the catalysis itself rather than catalyst characterization has been the main focus of Cu-Beta studies.[42−44] As such, the discussion on zeolite Beta shall be brief and limited to correlating structurally relevant

Table 1. Characterization Techniques Commonly Used for the Interrogation of Cu-Zeolites, Including Their Associated Strengths and Limitations

technique	strengths	limitations
XRD[61−65]	atomic resolution	lack of short-range sensitivity
	Cu ion location with respect to zeolite structure	averaging over partially occupied Cu positions
	sensitive to structural changes at the unit cell level (changes in bond distances)	limited by reciprocal space
XAS[66,67]	atomic resolution	long-range sensitivity (limited to ∼5 Å around the absorbing atom)
	Cu oxidation state	averaging over Cu in multiple environments and oxidation states
	Cu coordination geometry	
EPR[68−71]	sensitive to paramagnetic species	typically requires low temperatures
	can probe multiple Cu cation local environments	highly sensitive to the presence of water and paramagnetic impurities
	indirectly Cu oxidation state	not sensitive to diamagnetic species (e.g., Cu^+ is EPR silent)
UV−vis−NIR[68,69,72]	sensitive to specific electronic environment	no atomic resolution
	"fingerprint" regions of particular transitions → ligand field environment	environment probe limited to the ligand field
	fast acquisition	presence of multiple components (e.g., at high metal loadings requires deconvolution)
FTIR[69]	"fingerprint" regions of specific molecular vibrations	no atomic resolution
	fast acquisition	indirect probing of the Cu environment based on the behavior of the probe molecules
	reaction intermediates probing	
TPR	quantify species with different redox states	no structural information
	heterogeneity of a reducible material	no atomic resolution
XPS	surface-sensitive	necessity of ultrahigh vacuum conditions
	accurate elemental composition	in situ characterization not possible
	chemical and electronic state of elements probed	

studies on Cu-Beta to a proposed interaction of the active sites therein.

3. EXPERIMENTAL TOOLS TO STUDY METAL-CONTAINING ZEOLITE CATALYSTS

A major contribution in the development of metal-containing zeolite catalysts for catalytic processes has been the thorough characterization of active sites within these porous materials. The ordered and well-defined crystalline lattices of zeolites, on one hand, make it possible to perform various spectroscopic studies into the nature (oxidation and coordination environment) of ions and species interacting with the framework itself. On the other hand, the combination of a reactive framework and multiple possible (metal) cationic sites often renders the direct probing of active sites and subsequent mechanistic insight difficult to obtain. Needless to say, there has been much debate on the nature of the active species in the SCR reaction. Narrowing it down to Cu-zeolites, after decades of study, the scientific community is yet to agree on the nature and role of Cu species stabilized inside these zeolite pores and their role in the NO_x conversion. Dimeric Cu species, isolated Cu^{2+} ions, and even CuO have been proposed to be active sites for the SCR reaction.[6,7,17,45−47] The importance of a Cu^+/Cu^{2+} redox functionality has also been stressed.[48−50] Knowing the nature and properties of the active Cu-containing site, of course, is the first stage in understanding the reason behind catalytic activity and therefore provides a platform from which better catalysts can be developed and eventually "designed". Nonetheless, there is yet a lot to learn about the dynamic behavior and accessibility of the active site within the support and multiple possible reasons why eventually such a catalyst deactivates.

Developments toward the characterization of catalytic solids under realistic reaction conditions have gone a long way to help us answer these questions. In addition to the development of conventional laboratory instrumentation, modern synchrotron radiation facilities with dedicated beamlines to study solid−gas interfaces have been pivotal toward the characterization of such materials and heterogeneous catalysts in general. A recent *Chemical Society Reviews* themed issue on the in situ characterization of heterogeneous catalysts provides a great overview of some of these developments realized in the past few years.[51] Two key aspects, as also highlighted in this issue, have been the improvement in the available time and spatial resolution of spectroscopic and scattering techniques toward the characterization of these materials, largely through the application of brighter radiation sources and more sensitive detectors. The possibilities of combining multiple complementary techniques both at laboratories and at synchrotron radiation sources to study powdered catalysts have provided a powerful tool kit to study catalyst materials in great detail.[52−54] Even more recently, a dedicated *ACS Catalysis* issue was focused on the emergence of in situ and operando techniques for the study of catalytic phenomenon. On the basis of both heterogeneous and homogeneous catalysts, the issue compiles recent advances in spectroscopic and microscopic[55] techniques to study catalytic processes "in action". Within the realm of heterogeneous catalysis, the issue focuses on the elucidation of active site(s) with a drive toward increasing studies performed under operando conditions[56,57] and with the combination of multiple techniques.[58−60] Table 1 lists the strengths and limitations of both synchrotron- and laboratory-based characterization tools used in the study of metal-exchanged zeolites. The same techniques have been used to obtain the results that are discussed further in the text.

4. CU SPECIES IN ZEOLITES FOR NH_3-SCR

The dispersion of TMI species in zeolites is influenced by several factors, such as the Si/Al ratio of the zeolite, the type of metal salt used to load the zeolites, the medium of exchange, and the pretreatment of the parent and as-prepared material, which are beyond the scope of this article. Details regarding the respective roles that these factors play have been summarized in review articles.[6,7] Since XRD is the most widely accepted technique for the determination of zeolite structures and location of extra-framework cations within zeolite structures, each subsection henceforth will begin with the results from crystallographic studies performed for elucidating the position of Cu cations within zeolites Y, ZSM-5, and SSZ-13. As demonstrated in the literature, the geometric and electronic characteristics (i.e., the "spectroscopic signature" of a TMI in a zeolite) is a combination of its crystallographic position and the number of Al^{3+} atoms in the neighboring environment.[73−75] Therefore, although crystallographic results present an average position for the TMI based on all the possible (distorted) locations, spectroscopic signatures will change for the same crystallographic position as a consequence of differences in the immediate surrounding environment. As such, discrepancies are often found for all the cation positions represented crystallographically and that reported on the basis of the spectroscopic data. Therefore, following the crystallographic locations, studies further related to the local environment of the Cu species and their interactions thereof with probe molecules or NH_3-SCR reactants are presented. Finally, the discussion highlights the active sites within the zeolite structures as proposed by in situ experiments.

4.1. Cu Species within Zeolite Y. *Crystal Structure and Cu^{2+} Cation Location.* Figure 3 illustrates the crystal structure of FAU with the corresponding cation locations for Cu^{2+} ions in zeolite Y. Zeolite Y is a three-dimensional large pore zeolite made up of *d6r* and *sod* composite units. The "cage-type" structure of the FAU framework renders it possible to include molecules with a spherical diameter of up to 11.24 Å within the supercage. The size for diffusion along the three axes of the cages, however, is limited to 7.35 Å. Several studies have been performed on Cu-Y using X-rays and neutrons on hydrated and dehydrated structures using both partially and fully exchanged samples. For the sake of simplicity, we shall consider Cu sites in SI′, SII, and SIII.[76−80] Sites I′ and II are present on the 6-membered rings of the sodalite cavity, with the former being part of the *d6r* subunits. Site III is located in the supercages of the structure. It is worth noting that site SIII is present only for low Si/Al ratios, that is, for zeolite X, which also has the FAU structure.[81] However, as discussed later in this section, much of the past literature on NH_3-SCR over Cu-Y zeolites have proposed the location of Cu in site SIII as crucial and as the active sites for the reaction, and therefore, it is considered in our study. It is also worth noting here that in two sequential studies, Bordiga et al. could show that because of its location between sodalite cavities, site SI′ is not accessible to CO or N_2 but is accessible to H_2.[82,83]

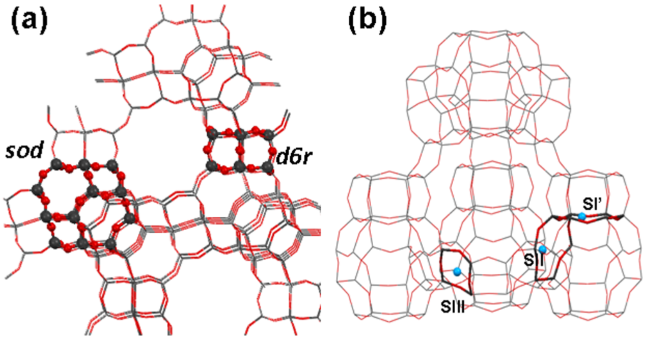

Figure 3. (a) Crystal structure of the FAU framework with the corresponding composite units represented as "balls and sticks" to highlight their position in the structure. (b) Crystallographic positions for Cu (blue balls) in zeolite Y (FAU framework), as proposed from single crystal and powder XRD studies. The structure is generated on the basis of the crystallographic information available in the literature.[79,84] SI′ lies on the face of the *d6r* subunits, next to sodalite cavities of the FAU structure. Site SII is present on the 6-membered ring faces of the sodalite cavities. SIII is located on 4-membered rings facing the supercages. Note: The bold sticks highlight the local environments of Cu in the structure.

Local Environment of the Cu^{2+} Cations As Influenced by the Zeolite Framework. Pierloot et al. performed EPR and ab initio cluster calculations on Cu^{2+}-exchanged zeolites A (LTA), Y (FAU), and ZK-4 (LTA). The results indicated the interaction of Cu with four framework oxygen atoms.[73] The authors could also demonstrate that in zeolites with a lower Si/Al (e.g. zeolite A), Cu would closely coordinate with two oxygen atoms (∼1.9 Å), followed by another O atom at ∼2 Å and, finally, a fourth oxygen at 2.2 Å. However, with increasing amounts of Si and, thereby, a lower propensity of Al^{3+}, the interaction is different with three close Cu−O distances (∼1.95−2.0 Å) and a fourth distant oxygen at ∼2.4 Å. Considering the issue of hydrothermal stability in the SCR reaction, zeolites with higher Si/Al ratios are preferred. Therefore, we shall consider the latter model as applicable. An illustration of this shifted position is presented in Figure 4. Recent single crystal studies performed on Cu-Y also support this theory.[79] The study showed that at site II, Cu coordinates with three close oxygen atoms at 1.85−2.0 Å and a fourth distant oxygen at ∼2.5 Å. The resulting structure is a distorted square-planar Cu^{2+} positioned closer to one side of the 6-membered ring unit.

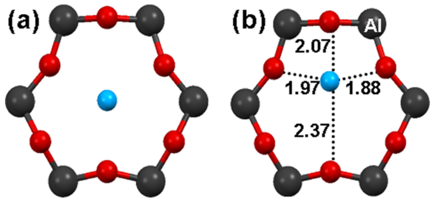

Figure 4. Cu^{2+} local environment in 6-membered rings of zeolite Y. (a) Initial crystallographic model showing the position of Cu^{2+} in the center of the 6-membered ring. Shifted position of Cu^{2+} in the 6-membered ring based on EPR spectra and ab initio calculations considering the location of one Al atom in the 6-membered ring. The local environment is a result of a distortion of the ring as well as a shift of the Cu^{2+} to achieve a distorted planar coordination. The distances shown are based on combined EPR and ab initio calculations reported in the literature.[73] The same can be considered for Cu-SSZ-13, in which the Cu^{2+} ions are located on the 6-membered ring planes as part of the *d6r* subunits.

Interaction with Probe Molecules and NH_3-SCR Reactants. Early FT-IR and EPR studies performed by Lunsford and coworkers showed that in zeolite Y, Cu formed tetraamine complexes in the presence of NH_3 and O_2 up to temperatures of 180 °C.[85,86] This observation was subsequently made in the presence of additional NO in the feed, and the authors proposed the formation of this complex as an active reaction intermediate for the SCR reaction; the reaction was proposed to proceed via an organometallic homogeneous-type complex formed within the zeolite pores.[25] Delabie et al., however, could conclude otherwise on the basis of in situ UV−vis−NIR spectroscopy combined with density functional theory (DFT) calculations. The authors observed a similar tetraamine complex; however, the

Cu^{2+} maintained coordination with at least one framework oxygen. Although the study was not performed under SCR conditions, a similar local environment could be postulated for the SCR reaction, in which the coordination of Cu to the zeolite lattice would be rather crucial. FT-IR studies performed by Howard and Nicol on Cu-Y accounted for the presence of CO (as a probe for Cu ions) in addition to NH_3 in their system.[87] In addition to the already identified Cu−amine complex, the authors further established the interaction of NH_3 with hydroxyl groups of the zeolite framework. Furthermore, upon evacuation of NH_3, the authors reported that the amounts of Cu−amine complexes in their system increased, indicating a higher affinity of NH_3 toward the Cu sites as compared with the hydroxyl groups. However, in the presence of CO, the authors postulated the formation of a $CuCO(NH_3)_n$ complex accompanied by a reduction of the Cu.

Lamberti et al. performed XAS and UV−vis−NIR studies on a Cu^+−Y sample prepared by a gas phase reaction between HY and CuCl. The resulting material was reported to possess Cu^+ ions exclusively within the structure. Interaction of these Cu^+ ions with CO resulted in the formation of metallic Cu for about 10% of the sample. In subsequent work, the same group performed XRD, XAS, and FT-IR experiments on a Cu-Y sample prepared in the same gas-phase manner as stated above.[81] The authors could locate the Cu^+ cations in sites SI′, SII, and SII′ (which is attributed as SII, but slightly positioned toward the sodalite cavities). The authors observed a significant migration of the Cu^+ into the supercages of zeolites Y upon exposure to CO. The same migration, however, was not observed in the presence of NO, since it is a weaker base than CO. Nonetheless, the authors postulated the formation of both mono- and dinitrosyl complexes being formed in sites SII′ and SII, respectively.

The studies above showed the possible location of Cu^+ ions in the supercages of zeolite Y resulted in a high mobility for the cations and could have both beneficial and adverse effects. On one hand, favorable species (as suggested) could be formed as a result of the interaction with NH_3. However, it should be noted that formation of a strong complex could result in a "blocking effect" on the active sites. On the other hand, the high mobility resulted in a migration of the Cu^+ ions away from their initial coordination with the lattice oxygen atoms. For example, under reducing environments, such as CO (one of the components in truck exhaust), the Cu ions were seen to migrate from their known positions into the supercages, thereby forming competing complexes or even metallic clusters; the latter is known to not favor the SCR reaction.[7,12] It is, however, very important to note that the local environment of Cu^+ could differ from that of Cu^{2+} within the zeolite framework, and therefore, slight discrepancies could be expected in bond distances or the coordination geometry when considering either ionic species.

Active Sites in Cu-Y. Early studies performed on Cu-Y by Kieger et al. proposed two types of active sites present in their catalysts.[88] Below 277 °C, the authors proposed Cu ions, of $[Cu-O-Cu]^{2+}$ nature, to be the active sites stabilized by NH_3 present in the supercages (site SIII); the assignment of the species was based on UV−vis−NIR data. However, such species in the supercages of zeolite Y had not been irrefutably identified, and the authors proposed the presence of Cu ions in close proximity in sites SII and SIII. A similar observation of Cu occupancy in site SII and SIII with the formation of Cu-oxo species was made by Iwamoto et al., although this study dealt with direct decomposition of NO.[89] As stated earlier, site SIII in the FAU structure is not always occupied by Cu ions. Therefore, although the local Cu environment could be accurately determined, the use of only UV−vis−NIR limited the approach to speculation on the exact location of Cu within the zeolite structure. Nonetheless, on the basis of FT-IR data, Kieger et al. proposed the reaction to proceed further via a $Cu^{2+} \leftrightarrow Cu^+$ redox cycle, where Cu^+ is oxidized in the presence of NO + O_2. The authors also postulated that above 327 °C, all Cu ions became active for SCR. In this study and another subsequent work, the authors reported the formation of CuO clusters and Cu ions in small (sodalite) cages within the FAU structure as the origin of unwanted N_2O in their system.[90−92] Subsequent studies by the same group showed, using catalytic data and TPR, that by "blocking" the sodalite cavities using various cocations (e.g., Ca, Ba, and lanthanides), the Cu-Y system could be active at lower temperatures (by ∼150 °C) and could avoid the formation of N_2O.[93] This further allowed the authors to introduce a higher content of Cu within the zeolite Y pores, thereby increasing the presence of Cu in the supercages and the formation of dimeric $[Cu-O-Cu]^{2+}$ species.

In a follow-up investigation, Delahay et al. also demonstrated a direct dependence on the amounts of H^+ (versus Na^+) as a countercation on the SCR activity.[94] This was a very crucial find, since H^+, Na^+, and NH_4^+ are the most commonly present counter cations in parent zeolites. Although close attention is given to the amounts of active TMI or the Si/Al ratios of a zeolite, the additional presence charge that is balancing counter cations is not often considered. The study illustrated that the increasing presence of H^+ instead of Na^+ increased low temperature activity. On the basis of FT-IR and TPR, the effect was explained by an increased migration of Cu from the "hidden" sodalite cavities to the more accessible SIII sites in the supercages as a consequence of replacing H^+ for Na^+. Quantum mechanical calculations could then demonstrate that in the presence of Na^+, Cu behaved more like an alkali cation, whereas in the presence of H^+, it behaved more like a TMI. Therefore, the redox process of $Cu^+ \leftrightarrow Cu^{2+}$ (which the authors considered as rate-determining) could occur faster in the presence of protons. Unfortunately, further structural characterization was not performed on the same systems, although this could have helped greatly in the understanding of the important issue of Cu mobility among the different subunits or sites within the zeolite structure. From an active site point of view, the multiple cation locations in zeolite Y make it rather challenging to directly probe active sites. The literature suggests, however, that $[Cu-O-Cu]^{2+}$ species are the active NH_3-SCR species within zeolite Y.

4.2. Cu Species within Zeolite ZSM-5. *Crystal Structure and Cu^{2+} Cation Location.* Figure 5 illustrates the crystal structure of MFI with the corresponding cation locations for Cu^{2+} ions in ZSM-5. ZSM-5, a medium-pore zeolite is a three-dimensional structure made up of *mor*, *cas*, *mel*, and *mfi* composite units. The "channel-type" structure of the MFI framework limits the maximum size of inclusions to 6.36 Å. ZSM-5 has a "zigzag" channel system; the larger channels along the *a*-axis allow diffusion of molecules up to 4.7 Å, and the smaller channels along the *b* and *c* axes, up to 4.46 Å in size. On the basis of XRD studies, Mentzen and Bergeret could locate five different cationic positions for Cu in the ZSM-5 structure.[95] Sites Cu1, Cu3, and Cu3′ in the ZSM-5 structure appear in the 5- and 6-membered ring subunits of the zeolite structure, which do not intersect with the main channels of ZSM-5. Sites Cu2 and Cu2′, which could account for ∼60% of the total Cu content, were found in the vicinity of the 10-membered ring windows of the structure. It was therefore proposed that these two sites might have

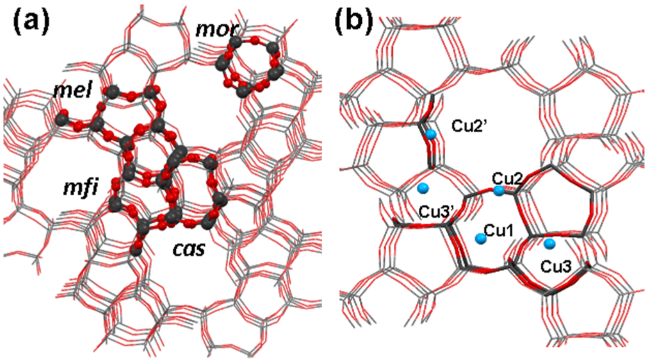

Figure 5. (a) Crystal structure of the MFI framework with the corresponding composite units represented as "balls and sticks" to highlight their position in the structure. (b) Crystallographic positions of Cu^{2+} (blue balls) in ZSM-5 (MFI framework) as proposed from single crystal XRD studies. The structure was generated using crystallographic information provided in the literature.[95] Sites Cu1, Cu3, and Cu3′ are present in 5- and 6-membered ring units of the structure. Sites Cu2 and Cu2′ (which together account for ~60% of the total Cu content) are located on the face of the channel system of the structure. Note: The bold sticks highlight the local environment of Cu^{2+} in the structure.

a significant role to play in catalysis considering their position closer to the large channels of the zeolites and their higher occupancy.

Local Environment of the Cu^{2+} Cations As Influenced by the Zeolite Framework. The local Cu geometries in Cu-ZSM-5 are slightly difficult to address due to the complex composite units that make up the structure as illustrated in Figure 5. Unlike zeolite Y, the cation sites are not positioned in defined subunits, rather in a combination of various 5- and 6-membered rings of the zeolite structure. Nonetheless, combinations of density functional theory (DFT)/ab initio calculations with EPR results have allowed the determination of Cu coordination geometry in some of these sites.[75] Generally speaking, the most relevant and agreed-upon sites for Cu cations (Cu2, Cu2′, and Cu3) in ZSM-5 are located in either the 10-membered ring channels or the channel interactions, and therefore, we shall consider the local environment for these three species. Figure 6 shows the crystallographic sites for Cu in zeolite ZSM-5 and compares it with the optimized local environment of Cu at sites Cu2, Cu2′, and Cu3. As in the case of Cu-Y, particular examples with one Al^{3+} per 5- or 6-membered ring is considered for discussion, since this would be most representative of a local environment within a zeolite with a high Si/Al ratio as favored in SCR.

The cations could be coordinated to 5- or 6-membered rings (in some cases (Cu2), to both), according to crystallographic locations. Compared with the crystallographic studies, cations Cu2 and Cu3 should be located in the as-labeled sites β and γ, respectively. Both are 6-membered ring sites, however, with additional O-T-O bridges. Cu's at these sites were shown to bind closely to four lattice oxygen atoms, with an average distance of 1.95 Å (the exact distances are presented in Figure 6). The Cu2′ site from the crystallographic studies was located in a 5-membered ring structure. The comparable 5-membered ring environment from the EPR/DFT study was labeled as site δ. Cu at this site was found closely coordinated to two oxygen atoms at ~1.93 Å and two distant oxygen atoms at ~2.02 Å. Therefore, similar to the case of Cu-Y, the local environment around the Cu cation appeared slightly different when analyzed with a technique more sensitive to the local arrangement of atoms around the Cu.

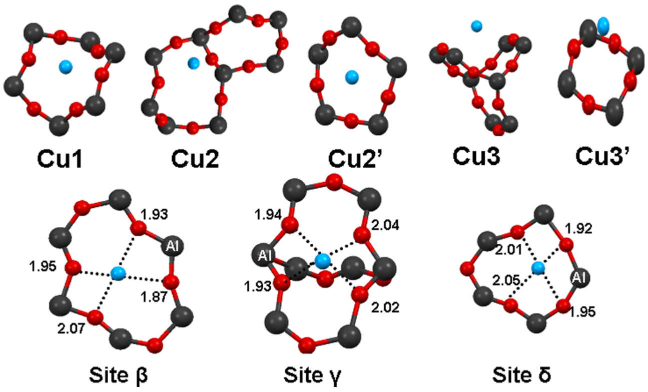

Figure 6. Cu^{2+} local environment in zeolite ZSM-5. Top: Local environments of sites Cu1, Cu2, Cu2′, Cu3, and Cu3′ from the crystallographic model is presented as a comparison. Sites β, γ, and δ correspond to the local environments of Cu2, Cu3, and Cu2′, respectively. The final bond distances are as obtained from EPR and ab initio calculations.[75] The position of Al^{3+} corresponds to models β4, γ5, and δ2 from the same work. The models presented here are merely a visual representation of the published work and are not original geometry optimized structures.

Interaction with Probe Molecules and NH_3-SCR Reactants . Lamberti et al. performed combined experiments on Cu-ZSM-5 samples prepared via gas phase exchange of CuCl salts into H-ZSM-5.[96] The idea of the preparative approach was to obtain well-dispersed and isolated Cu^+ ions, which the authors confirmed by their XAFS, UV−vis−NIR, FT-IR, and EPR results. To maintain the Cu^+ oxidation state, the sample had to be kept under vacuum when not exposed to probe gases (N_2, CO, and NO). Nonetheless, Lamberti and co-workers observed two types of Cu^+ species (labeled as families I and II in the study), both accessible via large channels. In addition to differing in the number of CO molecules either site could adsorb, the Cu cations did not appear to be mobile. More interestingly, adsorption of NO lead to NO decomposition (to N_2O) already at room temperature with formation of $Cu^{2+}(NO)(NO_2)$, which demonstrated the propensity of the Cu ions to oxidize under such environments.

In a subsequent study, Palomino et al. performed similar experiments on a Cu-ZSM-5 prepared via conventional wet ion exchange.[80] On the basis of FT-IR, the obtained Cu^{2+} species appeared to change coordination (rather than reduce) under vacuum dehydration treatments, up to 200 °C. Further heating to 400 °C though, led to gradual reduction of the Cu^{2+} species. Interestingly, in contast to the previous case, in which the authors managed to obtain only isolated Cu^+, the EXAFS data herein suggested the presence of Cu−O−Cu dimeric oxocations, highlighting the tendency of Cu ions in ZSM-5 (prepared by conventional techniques) to form Cu−O−Cu type species irrespective of their oxidation state and gas environment. Subsequent exposure to H_2O at room temperature was not seen to affect the oxidation state, but led to a change in the coordination environment and a decrease in the number of Cu−O−Cu species, as observed in EXAFS. However, exposure to O_2 in the presence of H_2O appeared to oxidize the Cu^+ and also led to the formation of Cu−O−Cu species alongside isolated Cu^{2+} species.

Neylon et al. studied the redox behavior of Cu in Cu-ZSM-5 using temperature-programmed reduction combined with XAFS spectroscopy.[97] The authors noted that initially, Cu^{2+} ions are located in two sites, namely, isolated Cu^{2+} and bridged

Cu—O—Cu clusters. The authors noted that reduction in H_2 resulted in migration of Cu (above 375 °C) to form small clusters, whereas exposure to CO resulted in a change in only the oxidation state, from Cu^{2+} to Cu^{+}. On the basis of EPR, Larsen et al. had pointed out two types of species in dehydrated Cu-ZSM-5: namely, square-pyramidal and square-planar sites.[98] The relative concentration of the former appeared to increase with increasing amounts of Cu. The species could sit on either 5- or 6-membered rings, with a preference for the former. The two types of species observed herein could be compared with those observed by Neylon and co-workers, that is, Cu—O—Cu type species on a 6-membered ring (or adjoining 6-membered rings) and the isolated Cu^{2+} ions in 5-membered rings. Additional theoretical calculations by Teraishi et al.[99] and Broclawik et al.[100] could also support this observation and in addition proposed the oxo species as more reactive than the lone pair Cu toward interaction with probe molecules, such as CO or NO.

Active Sites in Cu-ZSM-5. From their original series of studies in Cu-ZSM-5, Iwamoto et al. proposed the formation of paired Cu species bridged by oxygen atoms of Cu—O—Cu nature to be the active sites in the closely related HC-SCR and NO decomposition reactions.[19,101−103] This proposal was based on the observation that increasing amounts of Cu (Cu/Al > 0.2) led to higher activity. This finding could be further explained by Groothaert et al., who reported the formation of a bis(μ-oxo)dicopper species at a Cu/Al ratio of 0.34 but not at a Cu/Al ratio of 0.14.[104] The detailed EXAFS/UV−vis−NIR/kinetic studies under NO decomposition conditions could directly probe these Cu cores. The advantage of performing such a combined study was the possibility to accurately elucidate the particular species involved in the reaction under in situ conditions. A similar observation was made by Da Costa et al. who proposed, on the basis of XAFS, the presence of isolated Cu^{2+} and Cu dimers $[Cu—O—Cu]^{2+}$ after calcination of Cu-ZSM-5.[105] The authors could also relate the increasing Cu/Al ratio (0.12−0.60) to an increase in the amount of Cu dimers, whereas the amounts of isolated Cu^{2+} started to level off.

Further EPR studies comparing different Cu-zeolites performed by Smeets et al. showed a direct dependence on the amount of bis(μ-oxo)dicopper in zeolite ZSM-5 and the superior catalytic activity of the system.[106] Krivoruchko et al. studied the electronic state of Cu under HC-SCR conditions and proposed otherwise. The authors proposed that below 1% wt loading, isolated octahedrally coordinated Cu^{2+} and Cu^{2+} associated with extra-framework Al^{3+} forming spinel-like structures were mainly present. The authors proposed these as the active sites in the SCR process when propane was used as a reducing agent. At wt loadings > 1%, they proposed the formation of nanocrystalline Cu-hydroxo type species, which were active only at temperatures higher than 300 °C. These studies were, however, performed ex situ, and the samples were unusually prepared by an incipient wetness impregnation method using $CuCl_2$ salts, which could explain the contradictory results observed.

The presence of $[Cu—O—Cu]^{2+}$ was also observed by Sachtler and co-workers in a series of "overexchanged" Cu-ZSM-5 catalysts. On the basis of FT-IR and EPR, the authors demonstrated the presence of Cu^{2+} dimers and isolated Cu^{2+} ions.[107,108] The dimers further formed the $[Cu—O—Cu]^{2+}$ species upon heating and in the presence of oxygen. On a similar "overexchanged" Cu-ZSM-5, Shpiro et al.[109] demonstrated the presence of both isolated and multinuclear (O-bridged) Cu species on the basis of XPS and stressed the predominance of the 2+ oxidation state of Cu during NO_x reduction conditions. Hamada et al., on the basis of XAFS studies, proposed the presence of isolated Cu^{2+} species, as opposed to CuO, Cu_2O, metallic Cu, Cu acetates, or hydroxide clusters.[110] The EXAFS studies in this case allowed them to elucidate the near neighbor atoms, and they reported the formation of Cu—Cu pairs only at higher Cu loadings. It should be noted, however, that the parent zeolite had a rather high Si/Al ratio of 35, thereby rendering the proximal location of two Cu ions as disfavored. Furthermore, it is difficult to unambiguously differentiate this component from the other higher-order shell components (i.e., zeolite contribution) in an EXAFS spectrum. Shelef had also proposed the role of square-planar isolated Cu^{2+} as active species in NO decomposition on the basis of EPR observations from earlier studies.[111] A detailed combined XPS and X-ray excited auger electron spectroscopy (XAES) study by Grünert et al. tested several Cu-ZSM-5 catalysts prepared by different methods, including excessive and controlled wet ion exchange, wet impregnation, solid state exchange, and physical mixtures.[112] The study concluded that the samples most active in propene-SCR contained both isolated Cu^{2+} in low symmetry environments and Cu clusters linked by extra-framework oxygen atoms.

The Cu environment in ZSM-5 is rather complex because the various coordination environments make it possible for a variety of Cu species to form. The method of introducing Cu ions no doubt plays a major role in the initial coordination environment of Cu found in these systems; however, in the presence of additional reactants, migration of Cu leads to further interaction with other Cu ions or oxygen atoms, leading to the formation of small clusters. In other words, depending on the degree of Cu exchange and the presence of oxygen in the system, both Cu^{2+} ions and $[Cu—O—Cu]^{2+}$ species can be considered as the predominant Cu species,[113−115] and most likely, both are active in SCR.

4.3. Cu Species within Zeolite SSZ-13.

Crystal Structure and Cu^{2+} Cation Location. Figure 7 illustrates the crystal structure of CHA with the corresponding unique cation location for Cu^{2+} ions in zeolite SSZ-13. SSZ-13 is a three-dimensional small pore zeolite made up of *d6r* and *cha* composite units. The "cage-type" system allows molecules up to 7.37 Å with limiting dimensions in the *a*, *b*, and *c* axes being 3.72 Å. Fickel et al. performed powder XRD studies on Cu-SSZ-13 to propose the location of the cations therein.[116] In contrast to the other

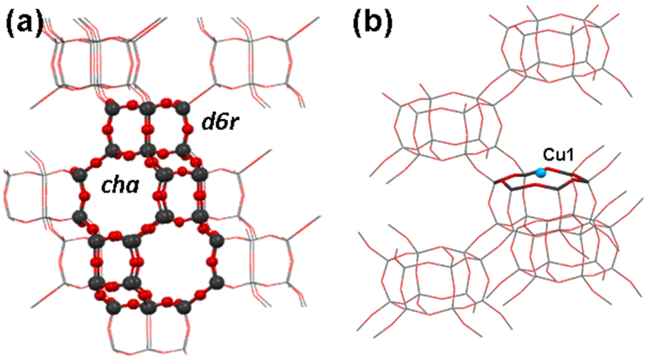

Figure 7. (a) Crystal structure of the CHA framework with the corresponding composite units represented as "balls and sticks" to highlight their positions in the structure. (b) Crystallographic position of Cu^{2+} (blue ball) in SSZ-13 (CHA framework) as proposed from powder XRD studies.[116] The unique location for Cu cations in this structure is on the plane of the *d6r* subunits facing the *cha* cavity. Note: The bold sticks highlight the local Cu^{2+} environment in the structure.

zeolites, Cu^{2+} is exclusively located on the face of the *d6r* units of the SSZ-13 structure after calcination. The authors also studied the same sample under increasing temperature conditions and could demonstrate that the location of Cu^{2+} does not change, even at elevated temperatures up to 600 °C.

Active Sites in Cu-SSZ-13. Recent studies performed by Korhonen et al. proposed isolated Cu^{2+} cations on the plane of *d6r* rings in Cu-SSZ-13 as active sites for the NH_3-SCR reaction on the basis of ex situ EXAFS and in situ UV−vis−NIR studies.[17] The comparative study showed that although Cu-ZSM-5 was active for both the SCR and NO decomposition reactions, Cu-SSZ-13 showed a higher SCR activity than Cu-ZSM-5, but no activity in NO decomposition. The Cu cations were located in the center of *d6r* units of the SSZ-13 structure, a unique site for Cu^{2+} in this zeolite. The above study further showed that the Cu^{2+} ions were shifted slightly toward the edge of the 6-membered rings, as illustrated in Figure 8. The reason for this discrepancy lies in the fact that the cation locations were determined using XRD, which is sensitive to the long-range order of materials. Highlighted as one of the drawbacks of XRD in Table 1, atomic positions with fractional occupancies such as that of Cu, in this case, are averaged over the whole sample. EXAFS, on the other hand, is sensitive to the local, real space environment (in this case, of the absorbing Cu-atom) and therefore could be used much more accurately to determine the local structure.

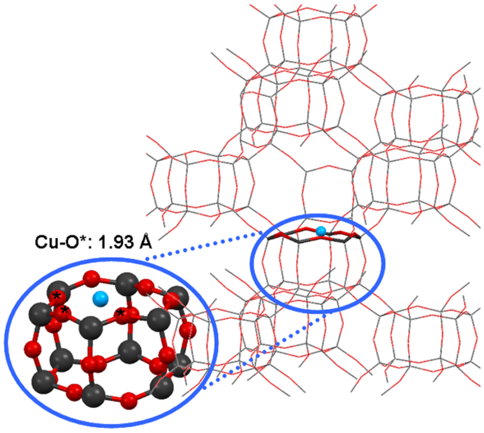

Figure 8. The local environment of Cu^{2+} in the *d6r* subunits of zeolite SSZ-13, which is proposed as the active site for the SCR reaction.[17,47] The nearest neighbor lattice O atoms have been labeled with an asterisk (*).

These findings were further confirmed by Deka et al. using combined XAFS/XRD studies, which could probe the location of Cu^{2+} ions on the plane of *d6r* rings of SSZ-13 as the active sites under SCR reaction conditions and temperatures.[47] The study demonstrated that at lower temperatures, a direct Cu−NH_3 interaction was observed, concurrent with lower activity of the system. At higher temperatures, though, Cu^{2+} was consistently located on the plane of the *d6r* subunits of the structure. Figure 9 illustrates the model showing the changing Cu local environment as a function of temperature. The authors in both cases did not observe a redox functionality for the active Cu sites, which has been proposed in the past as an important step, for the HC-SCR reaction.[48,49] More recently, Kispersky et al. performed comparative operando XAFS studies on Cu-SSZ-13, Cu-SAPO-34, and Cu-ZSM-5 under NH_3-SCR conditions.[50] The studies showed a mixture of Cu^{+} and Cu^{2+} species to be present in all three catalysts. The amount of Cu^{+} species at 200 °C under reaction conditions were 15%, 45%, and 65% for Cu-SSZ-13, Cu-SAPO-34, and Cu-ZSM-5, respectively. However, the authors also calculated the reaction rates per mole of Cu and could not correlate this with the amounts of Cu^{+} present. Further studies were performed by the same group integrating the XAFS studies with periodic DFT calculations on Cu-SSZ-13.[117] The combined studies suggested that in the presence of the "fast-SCR" reaction (i.e., 1:1 ratio of NO and NO_2 in the feed), Cu was present as exclusively Cu^{2+} species. However, under standard conditions, a mixture of 4-fold Cu^{2+} and 2-fold Cu^{+} were the most stable active species on the catalyst surface. The computation further suggested the 2-fold Cu^{+} coordinated with an additional water molecule as the key and stable species under standard SCR conditions. Although there is disagreement concerning the redox functionality of Cu species, as evidenced by the two studies presented above, the location of the monomeric Cu^{2+} ions on the 6-membered rings as active sites in Cu-SSZ-13 is consistent with evidence from literature. A recent work by Kwak et al. on Cu-SSZ-13 with increasing weight loadings of Cu in the samples, however, suggested that it is at lower weight loadings that Cu predominantly occupies the 6-membered ring sites. However, upon reaching higher than 60% weight loadings of Cu in the samples, TPR and FT-IR studies suggested the presence of a second Cu species located in the cages of the zeolite structure. The studies however, require further complementary evidence and characterization, since the observed

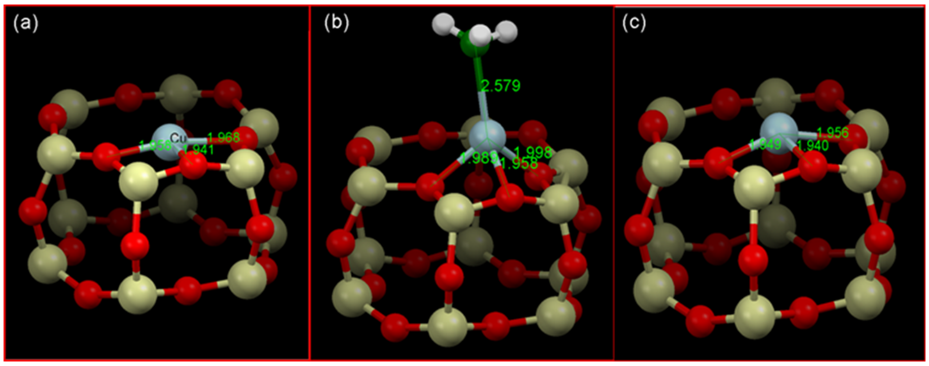

Figure 9. Illustrations of the local Cu^{2+} environment in *d6r* subunit of CHA.[47] (a) Local structure after calcination with Cu^{2+} on the plane and slightly distorted from the center of the *d6r* subunit of CHA; (b) interaction with NH_3 at ∼125 °C under SCR conditions resulting in a coordination geometry change; (c) under SCR conditions above 250 °C. The local environment is obtained from EXAFS fits using an initial model proposed from the refinement of the corresponding diffraction data collected at the different temperatures.

differences in the TPR and FT-IR profiles can be explained by the differences in, for example, Brönsted acidity or the presence of cocations, etc., as shown in studies performed with zeolite Y[93,94] or from the influence of extra-framework multinuclear Cu species, as shown recently with Cu-SAPO-34.[30]

Although the focus of this article was on zeolite-based catalyst materials, closely related silicoaluminophosphates, especially Cu-SAPO-34, have also been shown to be active in the SCR reaction, as evidenced in both patent and academic literature.[18,29,30,33] SAPO-34, although not a zeolite in the original sense, also possesses the CHA structure. Cu cations can be introduced into the structure via ion exchange or precipitation methods, and isolated Cu^{2+} species have been proposed as active sites in these catalysts on the basis of TPR and FT-IR.[18,30,118] A more direct proof from XRD studies on Cu-SAPO-34 prepared via direct synthesis also supported this conclusion and could show the location of isolated Cu^{2+} ions near the *d6r* subunits of the SAPO-34 structure. Compared with SSZ-13, however, these ions were located slightly away (~0.5 Å) from the plane of the 6-membered ring toward the cages of the structure. Nonetheless, Cu^{2+} ions appeared to have a preference for the location on the *d6r* units within CHA, and this appeared to have a positive effect on the catalytic performance of the system for SCR. It should also be noted, however, that the presence of additional Cu species (or a second site for Cu^{2+}) has been suggested within the SAPO-34 framework.[119,120] Wang et al. suggested that this could arise from either increasing the propensity of Al within the framework, therefore increasing the probability of near-neighbor Cu, which further generates CuO type species. More interestingly, as also suggested by Zamadics et al., Cu could locate at either site (III) or site (I) in the CHA structure, the former being in the center of the *d6r*, and the latter slightly off the plane and into the cages of the *d6r*. Therefore, the possibility of a second site for Cu^{2+} ions within the SAPO-34 framework cannot be completely ruled out; however, the proximity of the two sites rather suggests that Cu would be predominantly present in either one or the other site.

4.4. Cu Species within Zeolite Beta.

Crystal Structure and Cu^{2+} Cation Location. Zeolite Beta (BEA) possesses an intergrowth structure that renders it difficult to perform structural characterization to locate the position of TMIs within the structure. Typically, the structure is made up of three polymorphs named A, B, and C. The different polymorphs are obtained as a result of a different stacking order of the same central building layer stacked at different angles. The Cu-Beta structure presented herein is based on polymorph A; however, it is worth noting that from a more local perspective, the countercation environments of the different polymorphs would be comparable and similar to each other.[121] Therefore, the proposed cation positions herein can also be applied, for example, to polymorph B.

Lobo et al. performed NMR experiments in a Li^+-exchanged zeolite Beta and could propose cation exchange sites based on interaction (or lack thereof) with oxygen molecules.[122] The postulated sites, labeled herein as Cu1, Cu2, and Cu3, were present in either pentasil or 6-membered rings of the structure, as shown in Figure 10a. The NMR study had concluded that very few of the sites were actually accessible to oxygen. Since Cu-Beta shows reasonable activity in the deNO$_x$ reaction,[43,123] we would have to assume that structurally accessible sites are present. Therefore, Figure 10b presents a slightly different picture for the proposed positions of the Cu cations. Cu1 is presented in a structurally analogous 6-membered ring, but facing the 12-membered ring channel. Site Cu2 is presented in the same position. Site Cu3 was found to be too close to two framework oxygen atoms (Cu−O = 1.3 Å) and was therefore moved to the alternate location in a different 5-membered ring facing the 12-ring channel. This would allow for the position of Cu in accessible sites over which the catalytic process could take place. Interestingly, both sites Cu1 and Cu3 in the alternate model are in locations comparable to that of the planar arrangement within 6-rings of the SSZ-13 structure and could be proposed as active for the SCR reaction.

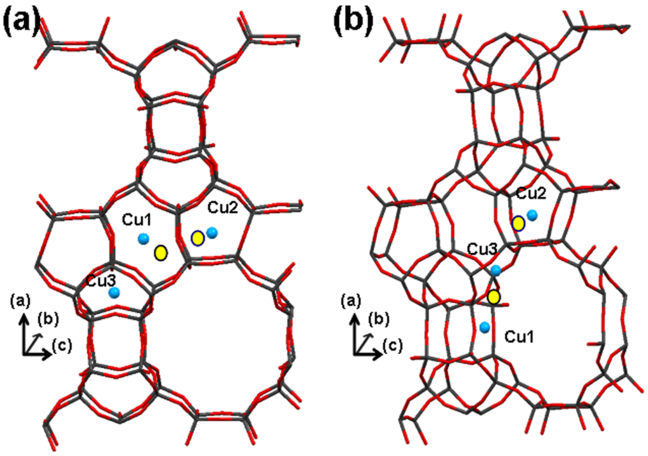

Figure 10. Cu cation position in Beta. Structure a is a proposal based on NMR experiments performed with Li^+ as a cation,[122] and structure b is an alternative proposal based on, and closely related to, structure a. Note: Blue balls represent the locations of the Cu cations, and the yellow circles represent a slightly shifted location to enable close coordination (~2 Å) with at least 3 oxygen atoms of the zeolite framework. The coordinates (a, b, and c) denote the axes of the unit cell.

Active Sites in Cu-Beta. Corma et al. performed combined XAES/XPS studies on Cu-Beta prepared at different exchange levels.[124] The study presented a direct correlation between the level of exchange, the $Cu^{2+} \leftrightarrow Cu^+$ redox process, and the catalytic activity of Cu-Beta catalysts. In overexchanged samples, the conversion between Cu^{2+} and Cu^+ was obtained much faster, and consequently, the catalysts were also seen to be more active. As such, a direct correlation between the ratio of Cu^+ to Cu (on the surface) and the catalytic activity could be established. Recently, De La Torre et al. concluded otherwise, suggesting Cu^{2+} to be the most active species in Cu-Beta on the basis of TPR experiments.[125] In contrast to the previous case, this particular study reported a decreasing NO$_x$ activity with increasing amount of Cu in the system. It should be noted, however, that both studies used a significantly different Si/Al ratio of the parent zeolite (11 for the former versus 25 for the latter). Logically, then, the amount of Cu present within the zeolite pores at ion exchange sites would be much higher in the former case (Si/Al: 11). On the contrary, an increasing amount of Cu in the latter (Si/Al: 25) could possibly result in the formation of clustered Cu species in the outer surface of the zeolite, which would not contribute toward the NH_3-SCR reaction.

Delahay et al. prepared Cu-Beta catalysts (Si/Al: 9.3) with different types of cocations present in the parent zeolite.[126] The study demonstrated that cocations play a very important role in the formation of various species within zeolite Beta. Within H-Beta, only CuO aggregates were found to be formed, whereas isolated Cu^{2+} species were formed mainly in Na-Beta at exchange levels lower than 120%. Similar to the observation made by Corma et al., the study concluded that the maximum activity was observed for samples, with a (113%) overexchange of Cu.

Dedecek et al. performed FT-IR and UV−vis−NIR experiments on a range of Cu-Beta catalysts, with varying counter cations and Si/Al ratios of the parent zeolite, and further tested them for NO decomposition activity. The study identified three Cu-type species in the prepared samples. Type 1 Cu species were found balanced by two close framework Al atoms, but were not active for NO decomposition. Type 2 species, found to be active in NO decomposition, were proposed to be single Cu ions balanced by one framework Al atom. Comparing with the NO decomposition activity of Cu-SSZ-13[17] and considering the number of framework Al atoms in the close vicinity of the Cu ions, type 1 species as denoted by Dedecek et al. could be attributed to isolated Cu^{2+} ions within the zeolite. Comparing further to the proposed cation sites herein, the type 1 species are possibly similar to Cu2 in Figure 10b. Type 2 Cu, however, would be susceptible to forming bis-μ-oxo type species, known to be very active for the NO decomposition reaction, as discussed earlier, and as was observed within Cu-Beta samples in other studies. [127] With respect to the cation sites presented herein, these species could be expected to form over sites Cu1 and Cu3 in Figure 10b, which are also in close vicinity to each other. Finally, at high concentrations of Cu, a type 3 species, attributed to Cu_2O, was formed, with negligible activity toward the NO decomposition reaction.

Cu-Beta is also known to produce unwanted N_2O, which has been attributed to clustered Cu-species[90] or, more recently, Cu aluminate type species.[29] On the basis of a single crystal XRD study, Attfield et al. had proposed positions for Cu^{2+} in zeolite mordenite similar to that presented herein.[128] In the same study, the authors could also note that the presence of water could significantly influence the migration of the Cu^{2+} species. Given the similarity of the local Cu environments, the comparable "channel type" structures of zeolite Beta and mordenite, and the presence of water as a product in the NH_3-SCR reaction, one could postulate the possible Cu ion migration within zeolite Beta, as well.

On the basis of XPS and XAES studies, Corma et al. also reported the migration of Cu species within Cu-Beta.[124] Depending on the oxidation state of the Cu ion, the study demonstrated a change in the surface Cu/Si atomic ratio, suggesting a dynamic migratory behavior of Cu ions in zeolite Beta. However, the authors observed that under reducing conditions, Cu^0 clusters were formed, which could not be reoxidized or redispersed. It should be pointed out, however, that in Cu-ZSM-5, the most populated sites are also located on the face of the 10-membered ring channels. The Cu-ZSM-5 system, however, does not appear to have such an extensive problem. Overall, Cu-Beta presents itself as a rather complex system for the study of active sites within.

As a result of the inherent disordered structure of the material, highly heterogeneous types of Cu species are formed within the zeolite channels, as discussed above and by others.[129] Furthermore, the high mobility of the Cu species therein allows for the formation of various species, which is not always seen to be reversible. Therefore, although active for the NH_3-SCR reaction, from a characterization point of view, the nature of Cu species within zeolite Beta appears difficult to control and thereby optimize to realize potentially very active materials for NH_3-SCR.

4.5. Rationalization of the Active Sites in the Cu-Zeolites. The nature and location of Cu^{2+} ions in the zeolite structure as discussed in the previous sections provides a good indication of the type of interactions made possible as a result of its location and environment within the zeolite framework. Spectroscopic studies have proved to be very helpful in determining the interaction of Cu-exchanged species with the zeolite framework. The role of each individual site, however, is rather challenging to address. In addition to other considerations, both reducibility and interaction of Cu sites within the various composite units can differ significantly as a consequence of the chemical softness of lattice oxygen atoms, the presence of Al^{3+} in the local vicinity of Cu, and the Si/Al ratio of the zeolite materials. Although the discussion of these effects is beyond the scope of this study, a general agreement can be found in the preference of zeolites with a high Si/Al ratios as favorable toward SCR. The underlying reason behind this is due to the inherent hydrothermal stability of systems with a high Si/Al ratio, a crucial requirement for active SCR catalysts. Perhaps less obvious is the indirect effect of high Si/Al ratios on the amount of isolated metal cations present in a zeolite. Zeolites with a high Si/Al ratio would be able to accommodate only a finite number of cations (e.g., Cu^{2+}) within the structure. Furthermore, the probability of more than one Al^{3+} (and therefore more than one cation) in close vicinity to each other is further reduced, resulting in well dispersed isolated metal species, which appear to be favorable toward a high catalytic performance. On the contrary, a high amount of Al^{3+} could possibly favor the proximal location of two cations and the formation of multinuclear Cu species, which does not appear to catalyze the SCR reaction.

Because of the lack of direct evidence, we exclude zeolite Beta from this section of the discussion. However, although speculative, the high activity of Cu-SSZ-13 as compared with Cu-ZSM-5 and Cu-Y can be explained in structural terms after consideration of the various subunits, Cu location, and studies performed to demonstrate the accessibility and mobility of the Cu ions at the various locations. In Cu-SSZ-13, Cu^{2+} cations are located on 6-member rings, part of the *d6r* structure and facing the *cha* cage. Cu−Cu interaction is not observed over the structure, which otherwise could result in the formation of dimeric species or Cu clusters.[17,47,116] However, the sufficiently large windows of the *cha* cage allow the diffusion of gas molecules in and out of the system. Furthermore, this still allows the Cu^{2+} cations enough mobility to interact with guest molecules within the cages. Figure 11 presents an illustration of the Cu active sites in Cu-SSZ-13 and interactions thereof as a function of temperature. Cu-ZSM-5, as evidence suggested, appeared to have two predominant Cu species.[104,105,112,130] Isolated Cu^{2+} ions were located

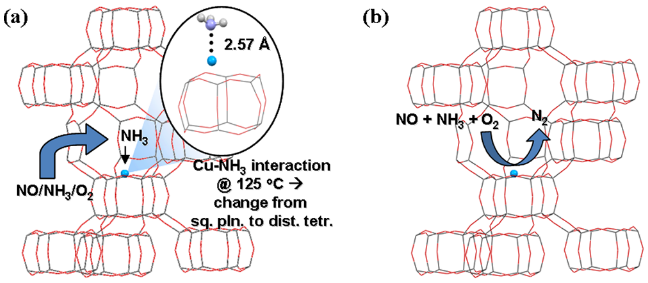

Figure 11. Rationalizing the Cu active sites in Cu-SSZ-13 as a function of temperature. (a) Cu-SSZ-13 at low temperatures (~125 °C). The Cu^{2+} site is easily accessible to all the reactant molecules because of the large windows of the *cha* cavity. A Cu−NH_3 interaction, leading to a change for Cu^{2+} geometry from square-planar to distorted tetrahedron appears to be predominantly present at these temperatures. (b) Cu-SSZ-13 at NH_3-SCR active temperatures. Cu^{2+} maintains its location on the plane of the *d6r* units. Reactant and product molecules do not have accessibility issues. Cu−Cu interactions are not observed.

in 5-membered rings of the structure, and $[Cu{-}O{-}Cu]^{2+}$ species (formed as a result of two proximal Cu) were found on 6-membered rings.[97,98]

Literature data suggest that the former species could be represented by Cu2′ in Figure 5, whereas the latter is formed on Cu2 and Cu3 sites. This is further illustrated in Figure 12 along with the proposed interactions as a function of temperature. With increasing Cu loadings and the presence of O_2 (the latter being present under SCR conditions), the O-bridged Cu species are favored as the isolated Cu^{2+} cations start to level off.[104,105] Both types of species are present in close proximity of the 10-membered ring channels and therefore do not suffer from issues of accessibility of guest molecules. Therefore, ZSM-5 shows very good activity in the SCR reaction. However, Cu-SSZ-13 turns out to be slightly better, which could be attributed to one of two reasons: (a) only isolated Cu^{2+} ions are active species (for NH_3-SCR), and therefore, the formation of O-bridged clusters does not support the SCR reaction but rather follows the NO decomposition pathway; or (b) the location of isolated Cu^{2+} ions in the 6-membered rings favors the low-temperature SCR activity, and at higher temperatures, all Cu species become active. Owing to the predominant presence of isolated Cu^{2+} ions in 6-membered rings, Cu-SSZ-13 exhibits the low temperature advantage.

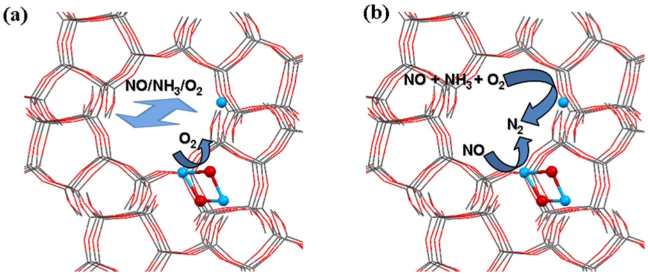

Figure 12. Rationalizing the Cu active sites in Cu-ZSM-5 as a function of temperature. (a) Active sites postulated for Cu-ZSM-5 in the vicinity of the 10-membered ring channel, allowing easy accessibility to all reactant molecules. Interaction of closely located Cu^{2+} cations with O_2 leads to the formation of bis-μ-oxo type species already at lower temperatures. (b) Proposed view of the Cu-ZSM-5 under "active" conditions. Cu bis-μ-oxo species are known active sites in NO decomposition, and one can expect the same reaction to occur over these sites. The isolated Cu^{2+} in 5-membered ring sites can be expected to be active for the NH_3-SCR reaction akin to that seen in Cu-SSZ-13.

Finally, zeolite Y has sites SI′, SII, and SIII populated with Cu^{2+} or Cu^{+} ions.[73,79,84] Site SI is akin to that seen in SSZ-13 and therefore should be postulated as a possible active site; however, the limiting dimensions of the sodalite cavity hindered movement of reactant molecules, as observed in the past.[82,83] Thereby, the site, although potentially active, is inaccessible to NO and NH_3. Site SII is located in 6-membered rings and therefore should be active at low temperatures, as per the arguments presented above. However, the Cu ions in this site have also been proposed to be highly mobile and tend to migrate into the supercages, losing coordination with the lattice oxygen atoms. The same could be postulated for site SIII. As proposed by Kieger et al., Cu−O−Cu type species could be formed over this site with neighboring Cu from site SII.[88] Thereby, the observed mobile character appeared to favor the formation of multiple Cu species and, eventually, the poor SCR activity. This is illustrated in Figure 13. Finally, a proposition of the behavior of different Cu species present in zeolite Beta and their possible role in NH_3-SCR is presented in Figure 14. The hypothesis is based on the limited studies available in the literature, as discussed in section 4.4.

In addition to the issues of Cu ion migration and clustering, in regard to the SCR reaction, there is the obvious consideration of deactivation due to hydrothermal conditions that are present in diesel exhaust streams. Although the current manuscript does not cover the nature of Cu sites in deactivated catalysts, a brief discussion of Cu environments in deactivated catalysts is worth noting. As stated earlier, the hydrothermal conditions in exhaust streams require the use of a catalyst that will be stable at temperatures as high as 700−800 °C, which can be challenging to achieve in zeolite systems. In addition, there is the problem of periodic temperature increase or temperature spikes related to the removal of soot by regeneration of the soot filters.[131] These temperature gradients have an obvious eventual detrimental effect on the catalysts, leading to catalyst deactivation.[132]

Earlier studies performed by Kucherov et al.[133] and Tanabe et al.[134] on Cu-ZSM-5 systems suggested that deactivated catalysts appeared to have isolated Cu^{2+} in slightly different local environments rather than formed clustered Cu species. Partial

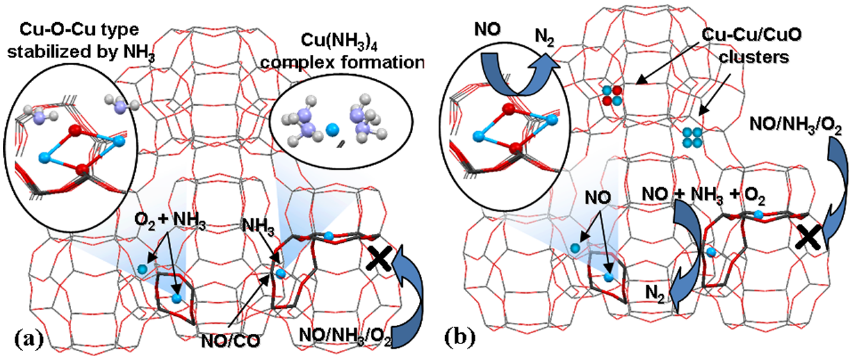

Figure 13. Rationalizing the Cu active sites in Cu-Y as a function of temperature. (a) Cu-Y at low temperatures. Cu^{2+} cations at site SI′ (*d6r* units) are inaccessible to reactant molecules because of the small windows of the *sod* cages. Cu^{2+} at site SIII has been proposed to form Cu−O−Cu type species stabilized by NH_3. Interaction with NO/CO results in slight movement of Cu^{2+} cations from 6-membered rings of the *sod* cavities (illustrated here in site SII). Interaction with NH_3 leads to the formation of tetraamine complexes in the cages of the zeolite. (b) Proposed view of Cu-Y at active temperatures. NO decomposition expected to occur over the Cu-oxo species. Cu^{2+} present at site SII (*sod* 6-membered ring) can be expected to contribute to the NH_3-SCR reaction. Finally, possible migration of Cu^{2+} ions, leading to the formation of clustered species in the supercages not active for NH_3-SCR.

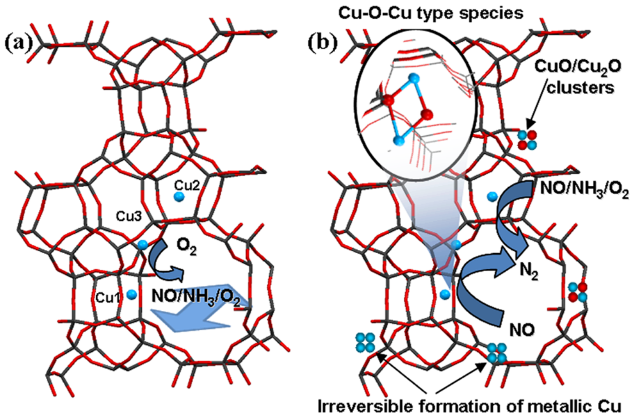

Figure 14. Proposition of the Cu active sites in Cu-Beta. (a) Interaction with various reactant molecules is not an issue within zeolite Beta because of the large channel system of the zeolite. (b) Interaction of vicinal Cu ions (Cu1 and Cu3) with oxygen can lead to the possible formation of Cu−O−Cu type species, observed in other systems. These sites are ideal for NO decomposition. High mobility of the Cu species presented within the zeolite can lead to the irreversible formation of metallic or oxidic Cu clusters, which are inactive for NH_3-SCR. Finally, isolated Cu^{2+} ions (Cu2) contribute to the NH_3-SCR reaction.

dealumination of the zeolite framework was suggested to play a role in changing the local geometry. Yan et al. had similar observations within Cu-ZSM-5, wherein they suggested the migration of Cu into Al_2O_3 or the formation of $CuAl_2O_3$ as the predominant Cu environments in deactivated catalysts.[135] Park et al. suggested that upon deactivation, Cu species in Cu-ZSM-5, which are originally present in either square-pyramidal or square-planar environments, migrate to form two additional distorted complexes that could not be further resolved.[136]

Even more recent studies from Kwak et al. compared Cu-Beta, Cu-ZSM-5, and Cu-SSZ-13.[137] The study concluded that although CuO or Cu aluminate type species form over Cu-Beta and Cu-ZSM-5, little changes are seen in the Cu species present in SSZ-13 catalysts. Thereby, it can be noted that even without significant migration to form bulk CuO or metallic Cu type species, Cu-zeolites can suffer a loss of activity upon exposure to hydrothermal conditions. Indeed, the isolated location of Cu-SSZ-13, with a reduced propensity of near-neighbor Cu ions could then be the root of the high stability seen in these systems. Further studies, however, need to be performed on deactivated Cu-zeolites to understand the multiple mechanisms that might play a crucial role within these systems.

5. CONCLUSIONS

Cu-exchanged zeolites are well-established catalytic materials for the abatement of NO_x from mobile sources. The nature and composition of the zeolite structure allows for the location of Cu at specific extra-framework cation sites, thus forming the catalytically active sites. The following concluding remarks can be made on the nature of these sites on the basis of the available literature.

- The local chemistry of Cu differs slightly within cation sites as a function of the presence of framework Al^{3+} in close vicinity. As was observed in the case of zeolite Y or SSZ-13, Cu tends to locate off the center of 6-membered ring planes to maintain close coordination with three lattice Os (and a distant O) in a square-planar environment. ZSM-5 has a rather diverse local environment for Cu cations composed of distorted 5- and 6-membered ring environments. The presence of multiple Cu types makes it rather challenging so as to be able to determine the local geometry of the systems, which have been observed as square-pyramidal, square-planar, or octahedral coordination, with a preference for the former two in dehydrated systems.
- Interaction of Cu in sites SII and SIII with various reactant gases in Cu-Y (e.g., NH_3) results in migration of these species into the supercages of the zeolite. These can further form Cu dimeric species of an oxidic or metallic nature. The limiting dimensions of the sodalite cages, on the other hand, render Cu present within these cages (site SI′) as inaccessible. Neither of the above-mentioned properties appears favorable toward NH_3-SCR.
- The Cu-active sites in Cu-ZSM-5 favor the formation of both isolated and Cu-oxo clusters (in oxygen-rich atmospheres), in close vicinity of the 10-membered ring channels of zeolite ZSM-5. The formation of the latter appeared to be favored because of the close proximity of two particular Cu cation sites. These species also dominate the zeolite pores with increasing amounts of Cu as the isolated Cu^{2+} species were seen to level off.
- Cu-SSZ-13 has a unique planar location for isolated Cu^{2+} in *d6r* units of the structure. Interaction with NH_3 under SCR conditions at temperatures below 125 °C changes the local geometry to distorted square-planar. The planar coordination on 6-membered rings of the zeolite structure is maintained under reaction conditions. Although the windows of the *cha* cages are large enough to allow passage of all reactant molecules, the formation of dimeric or clustered Cu species appears to be avoided over the framework.
- Comparison of the activity and selectivity of zeolites Y, ZSM-5, and SSZ-13 demonstrated that the isolated location of Cu^{2+} in planar 6-membered ring environments favors the SCR reaction, especially at low temperatures. The predominant presence of Cu^{2+} at these sites for SSZ-13 contributes to the low temperature activity demonstrated by the system, as compared with the other systems. In addition to isolated Cu^{2+}, Cu-ZSM-5 was found to have a predominant presence of Cu-oxo clusters, which are active in NO decomposition but do not necessarily contribute to NH_3-SCR. The propensity of Cu to cluster within the supercages of zeolite Y and inaccessibility of other sites seems to hinder activity in this system as compared with the others.
- The presence of a single site for Cu^{2+} in Cu-SSZ-13 also presents the system as a model system for further fundamental studies. The predominant presence of Cu^{2+} over one type of local environment would allow for the direct probing of structural and electronic effects using commonly available volume-averaged characterization tools.

■ AUTHOR INFORMATION

Corresponding Author

*E-mail: (B.M.W.) b.m.weckhuysen@uu.nl, (A.M.B.) a.m.beale@uu.nl.

Notes

The authors declare no competing financial interest.

■ ACKNOWLEDGMENTS

This research was carried out under Project No. M23.7.08301 in the framework of the Research Program of the Materials innovation institute M2i (www.m2i.nl). The authors also thank Bart Weiland and Frank Mertens (DAF Trucks) for fruitful discussions and advice. The authors also thank the referees for the valuable comments and corrections suggested which resulted in the improvement of this manuscript.

■ REFERENCES

(1) *NEC Directive Status Report 2008*, EEA Technical Report; European Environment Agency: Copenhagen, 2009.
(2) *NEC Directive Status Report 2010*, EEA Technical Report; European Environment Agency: Copenhagen, 2010.
(3) *NEC Directive Status Report 2011*, EEA Technical Report; European Environment Agency: Copenhagen, 2011.
(4) EU Commission. *Official Journal of the European Union* **2011**, *L 167*, 1.
(5) Klingstedt, F.; Arve, K.; Eränen, K.; Murzin, D. Y. *Acc. Chem. Res.* **2006**, *39*, 273.
(6) Centi, G.; Perathoner, S. *Appl. Catal., A* **1995**, *132*, 179.
(7) Brandenberger, S.; Krocher, O.; Tissler, A.; Althoff, R.; Kröcher, O. *Catal. Rev. Sci. Eng.* **2008**, *50*, 492.
(8) Parvulescu, V. I.; Grange, P.; Delmon, B. *Catal. Today* **1998**, *46*, 233.
(9) Hamada, H.; Haneda, M. *Appl. Catal., A* **2012**, *421*, 1.
(10) Roy, S.; Hegde, M. S.; Madras, G. *Appl. Energy* **2009**, *86*, 2283.
(11) Liu, Z.; Woo, S. I. *Catal. Rev. Sci. Eng.* **2006**, *48*, 43.
(12) Burch, R. *Catal. Rev. Sci. Eng.* **2004**, *46*, 271.
(13) Gabrielsson, P. L. T. *Top. Catal.* **2004**, *28*, 177.
(14) Korhonen, S. T.; Beale, A. M.; Newton, M. A.; Weckhuysen, B. M. *J. Phys. Chem. C* **2011**, 885–896.
(15) Bull, I.; Xue, W.; Burk, P.; Boorse, S.; Jaglowski, W. M.; Koermer, G. S.; Moini, A.; Patchett, J. A.; Dettling, J. C.; Caudle, M. T. Patent_Bull_CuCHA 1.pdf; U.S. Patent 7601662, 2009.
(16) Kwak, J. H.; Tonkyn, R. G.; Kim, D. H.; Szanyi, J.; Peden, C. H. F. *J. Catal.* **2010**, *275*, 187.
(17) Korhonen, S. T.; Fickel, D. W.; Lobo, R. F.; Weckhuysen, B. M.; Beale, A. M. *Chem. Commun.* **2011**, *47*, 800.
(18) Fickel, D. W.; D'Addio, E.; Lauterbach, J. A.; Lobo, R. F. *Appl. Catal., B* **2011**, *102*, 441.
(19) Iwamoto, M.; Hamada, H. *Catal. Today* **1991**, *10*, 57.
(20) König, A.; Held, W.; Richter, T. *Top. Catal.* **2004**, *28*, 99.
(21) Smelder, G.; Ahlstrom, G.; Fredholm, S.; Loof, P.; Marsh, P.; WInterborn, D.; Frost, J.; Walker, A. *SAE Technical Papers* **2010**, 950750.
(22) Breen, J. P.; Burch, R. *Top. Catal.* **2006**, *39*, 53.
(23) Shibata, J.; Shimizu, K.; Takada, Y.; Shichi, A.; Yoshida, H.; Satokawa, S.; Satsuma, A.; Hattori, T. *J. Catal.* **2004**, *227*, 367.
(24) Kamolphop, U.; Taylor, S. F. R.; Breen, J. P.; Burch, R.; Delgado, J. J.; Chansai, S.; Hardacre, C.; Hengrasmee, S.; James, S. L. *ACS Catal.* **2011**, *1*, 1257.
(25) Williamson, W. B.; Lunsford, J. H. *J. Phys. Chem.* **1976**, *80*, 2664.
(26) Li, Y.; Armor, J. N. *Appl. Catal.* **1991**, *76*, L1.
(27) Madia, G.; Koebel, M.; Elsener, M.; Wokaun, A. *Ind. Eng. Chem. Res.* **2002**, *41*, 4008.
(28) Bull, I.; Xue, W.; Burk, P.; Boorse, S.; Jaglowski, W. M.; Koermer, G. S.; Moini, A.; Patchett, J. A.; Dettling, J. C.; Caudle, M. T. Patent_BullBASF_CuCHA II_US2009.pdf; U.S. Patent 0285737, 2009.
(29) Deka, U.; Lezcano-Gonzalez, I.; Warrender, S. J.; Lorena Picone, A.; Wright, P. A.; Weckhuysen, B. M.; Beale, A. M. *Microporous Mesoporous Mater.* **2013**, *166*, 144.
(30) Wang, L.; Li, W.; Qi, G.; Weng, D. *J. Catal.* **2012**, *289*, 21.
(31) Ren, L.; Zhu, L.; Yang, C.; Chen, Y.; Sun, Q.; Zhang, H.; Li, C.; Nawaz, F.; Meng, X.; Xiao, F.-S. *Chem. Commun.* **2011**, *47*, 9789.
(32) Moliner, M.; Franch, C.; Palomares, E.; Grill, M.; Corma, A. *Chem. Commun.* **2012**, *48*, 8264.
(33) Andersen, P. J.; Bailie, J. E.; Casci, J. L.; Chen, H.; Fedeyko, J. M.; Foo, R. K. S.; Rajaram, R. R. JM CuSAPO-34, World Patent 132452, 2008.
(34) Devadas, M.; Krocher, O.; Elsener, M.; Wokaun, A.; Soger, N.; Pfeifer, M.; Demel, Y.; Mussmann, L. *Appl. Catal., B* **2006**, *67*, 187.
(35) Schwidder, M.; Heikens, S.; De Toni, A.; Geisler, S.; Berndt, M.; Brueckner, A.; Gruenert, W. *J. Catal.* **2008**, *259*, 96.
(36) Luo, J.; Hou, X.; Wijayakoon, P.; Schmieg, S. J.; Li, W.; Epling, W. S. *Appl. Catal., B* **2011**, *102*, 110.
(37) Devadas, M.; Krocher, O.; Elsener, M.; Wokaun, A.; Mitrikas, G.; Soger, N.; Pfeifer, M.; Demel, Y.; Mussmann, L. *Catal. Today* **2007**, *119*, 137–144.
(38) Grossale, A.; Nova, I.; Tronconi, E.; Chatterjee, D.; Weibel, M. *Top. Catal.* **2009**, *52*, 1837.
(39) Colombo, M.; Nova, I.; Tronconi, E. *Catal. Today* **2010**, *151*, 223.
(40) Metkar, P. S.; Harold, M. P.; Balakotaiah, V. *Appl. Catal., B* **2012**, *111*, 67.
(41) Kucherov, A. V.; Doronkin, D. E.; Stakheev, A. Y.; Kustov, A. L.; Grill, M. *J. Mol. Catal. A: Gen* **2010**, *325*, 73.
(42) Tokunaga, K.; Ogawa, H.; Ariga, K.; Aoyama, H. Bea Tosoh_2009.pdf, World Patent WO 2008/038422, 2009.
(43) Peden, C. H. F.; Kwak, J. H.; Burton, S. D.; Tonkyn, R. G.; Kim, D. H.; Lee, J. H.; Jen, H. W.; Cavataio, G.; Cheng, Y.; Lambert, C. K. *Catal. Today* **2012**, *184*, 245.
(44) Wilken, N.; Wijayanti, K.; Kamasamudram, K.; Currier, N. W.; Vedaiyan, R.; Yezerets, A.; Olsson, L. *Appl. Catal., B* **2011**, *111*, 58.
(45) Moretti, G.; Ferraris, G.; Fierro, G.; Jacono, M.; Morpurgo, S.; Faticanti, M. *J. Catal.* **2005**, *232*, 476.
(46) Dzwigaj, S.; Janas, J.; Gurgul, J.; Socha, R.; Shishido, T.; Che, M. *Appl. Catal., B* **2009**, *85*, 131.
(47) Deka, U.; Juhin, A.; Eilertsen, E. A.; Emerich, H.; Green, M. A.; Korhonen, S. T.; Weckhuysen, B. M.; Beale, A. M. *J. Phys. Chem. C* **2012**, *116*, 4809.
(48) Praliaud, H.; Mikhailenko, S.; Chajar, Z.; Primet, M. *Appl. Catal., B* **1998**, *16*, 359.
(49) Mathisen, K.; Nicholson, D. G.; Stockenhuber, M. *Phys. Chem. Chem. Phys.* **2009**, *11*, 5476.
(50) Kispersky, V. F.; Kropf, A. J.; Ribeiro, F. H.; Miller, J. T. *Phys. Chem. Chem. Phys.* **2012**, *14*, 2229.
(51) Weckhuysen, B. M. *Chem. Soc. Rev.* **2010**, *39*, 4557.
(52) Bentrup, U. *Chem. Soc. Rev.* **2010**, *39*, 4718.
(53) Foster, A. J.; Lobo, R. F. *Chem. Soc. Rev.* **2010**, *39*, 4783.
(54) Newton, M. a; van Beek, W. *Chem. Soc. Rev.* **2010**, *39*, 4845.
(55) Chenna, S.; Crozier, P. A. *ACS Catal.* **2012**, *2*, 2395.
(56) Zhang, C.; Grass, M. E.; Yu, Y.; Gaskell, K. J.; DeCaluwe, S. C.; Chang, R.; Jackson, G. S.; Hussain, Z.; Bluhm, H.; Eichhorn, B. W.; Liu, Z. *ACS Catal.* **2012**, *2*, 2297.
(57) Alayoglu, S.; Krier, J. M.; Michalak, W. D.; Zhu, Z.; Gross, E.; Somorjai, G. A. *ACS Catal.* **2012**, *2*, 2250.
(58) Tyo, E. C.; Yin, C.; Vece, M.; Qian, Q.; Kwon, G.; Lee, S.; Lee, B.; DeBartolo, J. E.; Seifert, S.; Winans, R. E.; Si, R.; Ricks, B.; Goergen, S.; Rutter, M.; Zugic, B.; Flytzani-Stephanopoulos, M.; Wang, Z. W.; Palmer, R. E.; Neurock, M.; Vajda, S. *ACS Catal.* **2012**, *2*, 2409.
(59) Patlolla, A.; Carino, E.; Ehrlich, S. N.; Stavitski, E.; Frenkel, A. I. *ACS Catal.* **2012**, *2*, 2216.
(60) Frenkel, A. I.; Rodriguez, J. A.; Chen, J. G. *ACS Catal.* **2012**, *2*, 2269.
(61) Rietveld, H. M. *J. Appl. Crystallogr.* **1969**, *2*, 65.
(62) McCusker, L. B.; Von Dreele, R. B.; Cox, D. E.; Louër, D.; Scardi, P. *J. Appl. Crystallogr.* **1999**, *32*, 36.
(63) Shankland, K. *J. Res. Natl. Inst. Stand. Technol.* **2004**, *109*, 143.
(64) David, W. I. F.; Shankland, K. *Acta Crystallogr. A* **2008**, *64*, 52.
(65) Harris, K. D. M.; Tremayne, M. *Chem. Mater.* **1996**, *8*, 2554.
(66) www.xafs.org (accessed June 2, 2012).
(67) Koningsberger, D. C.; Prince, R. *X-Ray Absorption: Principles, Applications, Techniques of EXAFS, SEXAFS and XANES*; Chemical Analysis: A Series of Monographs on Analytical Chemistry and Its Applications; Koningsberger, D., Prins, R., Eds.; John Wiley & Sons; New York, 1987; p 688.

(68) Delabie, A.; Pierloot, K.; Groothaert, M. H.; Schoonheydt, R. A.; Vanquickenborne, L. G. *Eur. J. Inorg. Chem.* **2002**, 515.
(69) Hunger, M.; Weitkamp, J. *Angew. Chem. Int. Ed* **2001**, *40*, 2954.
(70) Faber, R. J.; Rogers, M. T. *J. Am. Chem. Soc.* **1959**, *81*, 1849.
(71) Richardson, J. T. *J. Catal.* **1967**, *177*, 172.
(72) Schoonheydt, R. A. *Chem. Soc. Rev.* **2010**, *39*, 5051.
(73) Pierloot, K.; Delabie, A.; Groothaert, M. H.; Schoonheydt, R. A. *Phys. Chem. Chem. Phys.* **2001**, *3*, 2174.
(74) Smeets, P. J.; Woertink, J. S.; Sels, B. F.; Solomon, E. I.; Schoonheydt, R. A. *Inorg. Chem.* **2010**, *49*, 3573.
(75) Groothaert, M. H.; Pierloot, K.; Delabie, A.; Schoonheydt, R. A. *Phys. Chem. Chem. Phys.* **2003**, *5*, 2135.
(76) Maxwell, I. E.; de Boer, J. J. *J. Phys. Chem.* **1975**, *79*, 1874.
(77) Haniffa, R. M.; Seff, K. *Microporous Mesoporous Mater.* **1998**, *25*, 137.
(78) Fowkes, A. J.; Ibberson, R. M.; Rosseinsky, M. J. *Chem. Mater.* **2002**, *14*, 590.
(79) Seo, S. M.; Lim, W. T.; Seff, K. *J. Phys. Chem. C* **2012**, *116*, 963.
(80) Palomino, G. T.; Fisicaro, P.; Bordiga, S.; Zecchina, A.; Giamello, E.; Lamberti, C. *J. Phys. Chem. B* **2000**, *104*, 4064.
(81) Palomino, G. T.; Bordiga, S.; Zecchina, A.; Marra, G. L.; Lamberti, C. *J. Phys. Chem. B* **2000**, *104*, 8641.
(82) Bordiga, S.; Scarano, D.; Spoto, G.; Zecchina, A.; Lamberti, C.; Arein, C. O. *Vibr. Spectrosc.* **1993**, *5*, 69.
(83) Bordiga, S.; Garrone, E.; Lamberti, C.; Zecchina, A.; Arean, C. O.; Kazansky, V. B.; Kustov, L. M. *J. Chem. Soc. Faraday. Trans.* **1994**, *90*, 3367.
(84) Haniffa, R. M.; Seff, K. *Microporous Mesoporous Mater.* **1998**, *25*, 137.
(85) Flentge, D. R.; Lunsford, J. H.; Jacobs, P. A.; Uytterhoeven, J. B. *J. Phys. Chem.* **1975**, *79*, 354.
(86) Williamson, W. B.; Flentge, D. R.; Lunsford, J. H. *J. Catal.* **1975**, *266*, 258.
(87) Howard, J.; Nicol, J. M. *J. Chem. Soc. Faraday Trans. 1* **1989**, *85*, 1233.
(88) Kieger, S.; Delahay, G.; Coq, B.; Neveu, B. *J. Catal.* **1999**, *183*, 267.
(89) Iwamoto, M.; Yokoo, S.; Sakai, K.; Kagawa, S. *J. Chem. Soc., Faraday Trans.* **1981**, *77*, 1629.
(90) Delahay, G.; Coq, B.; Kieger, S.; Neveu, B. *Catal. Today* **1999**, *54*, 431.
(91) Suarez, S.; Martin, J.; Yates, M.; Avila, P.; Blanco, J. *J. Catal.* **2005**, *229*, 227.
(92) Arous, W.; Tounsi, H.; Djemel, S.; Ghorbel, A.; Delahay, G. *Surf. Sci.* **2005**, *158*, 1883.
(93) Kieger, S.; Delahay, G.; Coq, B. *Appl. Catal., B* **2000**, *25*, 1.
(94) Delahay, G.; Villagomez, E. A.; Ducere, J.-M.; Berthomieu, D.; Goursot, A.; Coq, B. *ChemPhysChem* **2002**, *3*, 686.
(95) Mentzen, B. F.; Bergeret, G. *J. Phys. Chem. C* **2007**, *111*, 12512.
(96) Lamberti, C.; Bordiga, S.; Salvalaggio, M.; Spoto, G.; Zecchina, A.; Geobaldo, F.; Vlaic, G.; Bellatreccia, M. *J. Phys. Chem. B* **1997**, *101*, 344.
(97) Neylon, M. K.; Marshall, C. L.; Kropf, A. J. *J. Am. Chem. Soc.* **2002**, *124*, 5457.
(98) Larsen, S. C.; Aylor, A.; Bell, A. T.; Reimer, J. A. *J. Phys. Chem.* **1994**, *98*, 11533.
(99) Teraishi, K.; Ishida, M.; Irisawa, J.; Kume, M.; Takahashi, Y.; Nakano, T.; Nakamura, H.; Miyamoto, A. *J. Phys. Chem. B* **1997**, *101*, 8079.
(100) Broclawik, E.; Datka, J.; Gilb, B.; Kozyrab, P. *Phys. Chem. Chem. Phys.* **2000**, *2*, 401.
(101) Iwamoto, M.; Yahiro, H.; Tanda, K.; Mizuno, N.; Mine, Y.; Kagawa, S. *J. Phys. Chem.* **1991**, *95*, 3727.
(102) Iwamoto, M.; Yahiro, H.; Mizuno, N.; Zhang, W. X.; Mine, Y.; Furukawa, H.; Kagawa, S. *J. Phys. Chem.* **1991**, *96*, 9360.
(103) Iwamoto, M.; Furukawa, H.; Mine, Y.; Uemura, F.; Mikuriya, S.; Kagawa, S. *J. Chem. Soc. Chem. Commun.* **1986**, *16*, 1272.
(104) Groothaert, M. H.; VanBokhoven, J. A.; Battiston, A. A.; Weckhuysen, B. M.; Schoonheydt, R. A. *J. Am. Chem. Soc.* **2003**, *125*, 7629.
(105) Da Costa, P.; Moden, B.; Meitzner, G. D.; Lee, D. K.; Iglesia, E. *Phys. Chem. Chem. Phys.* **2002**, *4*, 4590.
(106) Smeets, P.; Groothaert, M.; Vanteeffelen, R.; Leeman, H.; Hensen, E.; Schoonheydt, R. *J. Catal.* **2007**, *245*, 358.
(107) Lei, G. D.; Adelman, B. J.; Sárkány, J.; Sachtler, W. M. H. *Appl. Catal., B* **1995**, *5*, 245.
(108) d'Itri, J. L.; Sachtler, W. M. H. *Catal. Lett.* **1992**, *15*, 289.
(109) Shpiro, E. S.; Gruenert, W.; Joyner, R. W.; Baeva, G. N. *Catal. Lett.* **1994**, *24*, 159.
(110) Hamada, H.; Matsubayashi, N.; Shimada, H.; Kintaichi, Y.; Ito, T.; Nishijima, A. *Catal. Lett.* **1990**, *5*, 189.
(111) Shelef, M. *Catal. Lett.* **1992**, *15*, 305.
(112) Gruenert, W.; Hayes, N. W.; Joyner, R. W.; Shpiro, E. S.; Siddiqui, M. R. H.; Baeva, G. N. *J. Phys. Chem.* **1994**, *98*, 10832.
(113) Groothaert, M. H.; Lievens, K.; VanBokhoven, J. A.; Battiston, A. A.; Weckhuysen, B. M.; Pierloot, K.; Schoonheydt, R. A. *ChemPhysChem* **2003**, *4*, 626.
(114) Woertink, J. S.; Smeets, P. J.; Groothaert, M. H.; Vance, M. A.; Sels, B. F.; Schoonheydt, R. A.; Solomon, E. I. *Proc. Natl. Acad. Sci. U.S.A.* **2009**, *106*, 18908.
(115) Smeets, P. J.; Groothaert, M. H.; Schoonheydt, R. A. *Catal. Today* **2005**, *110*, 303.
(116) Fickel, D. W.; Lobo, R. F. *J. Phys. Chem. C* **2010**, *114*, 1633.
(117) McEwen, J. S.; Anggara, T.; Schneider, W. F.; Kispersky, V. F.; Miller, J. T.; Delgass, W. N.; Ribeiro, F. H. *Catal. Today* **2012**, *184*, 129.
(118) Ishihara, T.; Kagawa, M.; Hadama, F.; Takita, Y. *J. Catal.* **1997**, *169*, 93.
(119) Wang, J.; Yu, T.; Wang, X.; Qi, G.; Xue, J.; Shen, M.; Li, W. *Appl. Catal., B* **2012**, *127*, 137.
(120) Zamadics, M.; Chen, X.; Kevan, L. *J. Phys. Chem.* **1992**, *96*, 2652.
(121) Corma, A.; Moliner, M.; Cantín, Á.; Díaz-Cabañas, M. J.; Jordá, J. L.; Zhang, D.; Sun, J.; Jansson, K.; Hovmöller, S.; Zou, X. *Chem. Mater.* **2008**, *20*, 3218.
(122) Accardi, R. J.; Lobo, R. F. *Microporous Mesoporous Mater.* **2000**, *40*, 25−34.
(123) Corma, A.; Fornes, V.; Palomares, E. *Appl. Catal., B* **1997**, *11*, 233.
(124) Corma, A.; Palomares, A.; Marquez, F. *J. Catal.* **1997**, *170*, 132.
(125) La Torre, U.; Pereda-Ayo, B.; González-Velasco, J. R. *Chem. Eng. J.* **2012**, DOI: 10.1016/j.cej.2012.06.092.
(126) Delahay, G.; Coq, B.; Broussous, L. *Appl. Catal., B* **1997**, *12*, 49.
(127) Shimizu, K.; Maruyama, R.; Hatamachi, T.; Kodama, T. *J. Phys. Chem. C* **2007**, *111*, 6440.
(128) Attfield, M.; Weigel, S. J.; Cheetham, A. K. *J. Catal.* **1997**, *170*, 227.
(129) Kefirov, R.; Penkova, A.; Hadjiivanov, K.; Dzwigaj, S.; Che, M. *Microporous Mesoporous Mater.* **2008**, *116*, 180.
(130) Sarkany, J.; D'Itri, J. L.; Sachtler, W. M. H. *Catal. Lett.* **1992**, *16*, 241.
(131) Chen, K.; Martirosyan, K. S.; Luss, D. *Chem. Eng. Sci.* **2011**, *66*, 2968−2973.
(132) Yahiro, H.; Iwamoto, M. *Appl. Catal., A* **2001**, *222*, 163.
(133) Kucherov, A. V.; Gerlock, G. L.; Jen, H. W.; Shelef, M. *Catal. Today* **1996**, *27*, 79.
(134) Tanabe, T.; Iijima, T.; Koiwai, A.; Mizuno, J.; Yokota, K.; Isogai, A. *Appl. Catal., B* **1995**, *6*, 145−153.
(135) Yan, J.; Lei, G. D.; Sachtler, W. M. H.; Kung, H. H. *J. Catal.* **1996**, *161*, 43.
(136) Park, J.; Park, H. J.; Baik, J. H.; Nam, I.; Shin, C.; Lee, J.; Cho, B.; Oh, S. H. *J. Catal.* **2006**, *240*, 47.
(137) Kwak, J. H.; Tran, D.; Burton, S. D.; Szanyi, J.; Lee, J. H.; Peden, C. H. F. *J. Catal.* **2012**, *287*, 203−209.